TLR 2/1 interaction of pectin depends on its chemical structure and conformation

Jermendi, Éva; Fernández-Lainez, Cynthia; Beukema, Martin; López-Velázquez, Gabriel; van den Berg, Marco A.; de Vos, Paul; Schols, Henk A.

Published in:
Carbohydrate Polymers

DOI:
10.1016/j.carbpol.2022.120444

Publication date:
2023

Carbohydrate Polymers 303 (2023) 120444

Contents lists available at ScienceDirect

Carbohydrate Polymers

journal homepage: www.elsevier.com/locate/carbpol

TLR 2/1 interaction of pectin depends on its chemical structure and conformation

Éva Jermendi [a], Cynthia Fernández-Lainez [b,c], Martin Beukema [b], Gabriel López-Velázquez [e], Marco A. van den Berg [d], Paul de Vos [b], Henk A. Schols [a,*]

[a] Laboratory of Food Chemistry, Wageningen University, Bornse Weilanden 9, 6708, WG, Wageningen, the Netherlands
[b] Immunoendocrinology, Division of Medical Biology, Department of Pathology and Medical Biology, University Medical Center Groningen, Hanzeplein 1, 9713, GZ, Groningen, the Netherlands
[c] Laboratorio de Errores Innatos del Metabolismo y Tamiz, Instituto Nacional de Pediatría, Av. Imán 1, piso 9, col. Insurgentes Cuicuilco 04530, Ciudad de México, Mexico
[d] DSM Food & Beverages, Alexander Fleminglaan 1, 2613, AX, Delft, the Netherlands
[e] Laboratorio de Biomoléculas y Salud Infantil, Instituto Nacional de Pediatría, Av. Imán 1, piso 5, col. Insurgentes Cuicuilco 04530, Ciudad de México, Mexico

ARTICLE INFO

Keywords:
Citrus pectin
HILIC-MS
HPAEC
Methyl-ester distribution
Toll-like receptors
Immunomodulation

ABSTRACT

Citrus pectins have demonstrated health benefits through direct interaction with Toll-like receptor 2. Methyl-ester distribution patterns over the homogalacturonan were found to contribute to such immunomodulatory activity, therefore molecular interactions with TLR2 were studied. Molecular-docking analysis was performed using four GalA-heptamers, $GalA_7Me^0$, $GalA_7Me^{1,6}$, $GalA_7Me^{1,7}$ and $GalA_7Me^{2,5}$. The molecular relations were measured in various possible conformations. Furthermore, commercial citrus pectins were characterized by enzymatic fingerprinting using polygalacturonase and pectin-lyase to determine their methyl-ester distribution patterns. The response of 12 structurally different pectic polymers on TLR2 binding and the molecular docking with four pectic oligomers clearly demonstrated interactions with human-TLR2 in a structure-dependent way, where blocks of (non)methyl-esterified GalA were shown to inhibit TLR2/1 dimerization. Our results may be used to understand the immunomodulatory effects of certain pectins via TLR2. Knowledge of how pectins with certain methyl-ester distribution patterns bind to TLRs may lead to tailored pectins to prevent inflammation.

1. Introduction

The health effects associated with dietary fibers are more and more discussed in the literature, but mechanisms that could explain the effects are often still lacking. An obvious reason for that is the high diversity of dietary fibers in their structure and functionality. Moreover, dietary fibers used in research are often compared without appropriate characterization, causing numerous contradictions in the literature regarding their health effects (Ferreira, Passos, Madureira, Vilanova, & Coimbra, 2015; Ramberg, Nelson, & Sinnott, 2010). Some dietary fibers may play an important role in gut health by serving as fermentation substrates and energy sources for the gut microbiota (Brownlee, 2011; Montagne, Pluske, & Hampson, 2003). Upon fermentation, the microbiota will generate short-chain fatty acids (SCFAs) that, among other effects, may reduce inflammation by increasing the number of immunoregulatory cells in the gut (Scharlau et al., 2009; Smith et al., 2013). Nevertheless, beneficial effects of polysaccharides independently from SCFAs have been also reported (Breton et al., 2015; Weickert et al., 2011) including direct immune-modulating effects of fibers on immune cells, such as THP-1 monocytes, regulatory T cells (Treg) or effector T cells (Beukema, Faas, & de Vos, 2020; Vogt et al., 2014).

Several in vivo and in vitro studies have been performed on the immunomodulatory effects of dietary fibers (Beukema et al., 2021; Ramberg et al., 2010; Sahasrabudhe et al., 2018; Vogt et al., 2016). A large variety of different plant-derived polysaccharides such as glucans, mannans and pectins have been studied for their immune system activating and -inhibiting properties (Prado et al., 2020; Rösch et al., 2017; Sahasrabudhe, Dokter-Fokkens, & de Vos, 2016). Moreover, many pectin structural domains have been tested for their bioactivity including homogalacturonans, arabinogalactan type I and II, and

* Corresponding author.
E-mail addresses: eva.jermendi@wur.nl (É. Jermendi), c.fernandez.lainez@umcg.nl (C. Fernández-Lainez), m.beukema@umcg.nl (M. Beukema), glv_1999@ciencias.unam.mx (G. López-Velázquez), marco.berg-van-den@dsm.com (M.A. van den Berg), p.de.vos@umcg.nl (P. de Vos), henk.schols@wur.nl (H.A. Schols).

https://doi.org/10.1016/j.carbpol.2022.120444
Received 7 September 2022; Received in revised form 18 November 2022; Accepted 5 December 2022
Available online 10 December 2022

rhamnogalacturonans (McKay et al., 2021; Popov & Ovodov, 2013). The direct interaction of dietary fibers and the intestinal cells happens through interaction with the so-called pattern recognition receptors (PRRs) (Shibata et al., 2014). PRRs play a significant role in intestinal immune regulation, since they are responsible for recognizing exogenous molecules (Ferreira et al., 2015; Shibata et al., 2014). Toll-like receptors (TLRs) form such a family of PRRs, which play an essential role in the activation of innate immunity (Takeda & Akira, 2005) and proved to be involved in dietary fiber-induced immune signaling (Prado et al., 2020). Dietary fibers have a highly complex and diverse structure and therefore they can either activate TLRs to different extents (e.g., high DM lemon pectin (Vogt et al., 2016)), or inhibit TLR signaling and decrease intestinal inflammation (e.g., low DM lemon pectin (Sahasrabudhe et al., 2018)). Studies have shown that various pectins are able to inhibit TLR4 activation specifically in monocytes and dendritic cells which is suggested to be induced through RG-I or RG-II side chains (Ishisono, Yabe, & Kitaguchi, 2017).

Through TLR signaling, fibers have shown to have several beneficial effects, including reduced intestinal permeability and thereby better gut barrier function (Vogt et al., 2014; Vogt et al., 2016), promoting immune responses against pathogens (Vogt et al., 2013) as well as reducing intestinal inflammation (Sahasrabudhe et al., 2018). It has been demonstrated that the chemical differences such as the methyl-ester distribution over the homogalacturonan backbone (Beukema, Jermendi, van den Berg, et al., 2021), the side chains and the chain length in fibers such as pectins (Vogt et al., 2013; Vogt et al., 2014) can regulate immune effects. More information on the effect of the chemical structure of fibers on intestinal immunity is therefore important to understand and to predict the efficacy of dietary fibers (Sahasrabudhe et al., 2018; Vogt et al., 2013).

Pectin is a well-known soluble dietary fiber that has, both direct and indirect, nutritional and physiological health effects. Its biological properties have gained increased attention in the last decades (Gerschenson, 2017). Pectin is commonly used as a functional ingredient in the food industry due to its thickening and gelling capacity (Kjøniksen, Hiorth, & Nyström, 2005). Commercial pectin is mainly composed of a linear chain of α-1,4 D-galacturonic acid (GalA) units, called homogalacturonan (HG), which covers approximately 70–90 % of the pectin backbone and can be methyl-esterified at the GalA *O*-6 carboxyl group and, less commonly, be *O*-acetylated at the GalA *O*-2 or *O*-3 positions depending on the source (Voragen, Beldman, & Schols, 2001). Other domains of pectin are rhamnogalacturonan-I (RG-I) and RG-II. RG-I comprises 20–30 % of GalA in of the pectin structure (Voragen, Coenen, Verhoef, & Schols, 2009). The technological and biological properties of a pectin depend on its structural characteristics like monosaccharide composition, level and distribution of methyl-esterification, level of acetylation, molecular weight (Mw), presence, type and length of side chains, and conformation or spatial structure (Beukema, Jermendi, Schols, & de Vos, 2020; Voragen, Pilnik, Thibault, Axelos, & Renard, 1995; Voragen, 2004). Furthermore, the solubility of pectins increase with an increase of DM, while an increased pectin molecular weight decreases the solubility (Sila et al., 2009). Specific pectin structures can have therapeutic potential as they can modulate TLR signaling and in that way stimulate innate immune responses and protect against inflammatory diseases (Shibata et al., 2014). The level and distribution of methyl-esters over the pectin backbone are fundamental elements contributing to pectin's functionality (Sahasrabudhe et al., 2018; Vogt et al., 2016; Voragen et al., 2009). The percentage of methyl-esterified GalA residues over the backbone is defined as the degree of methyl-esterification (DM). The main methyl-ester distribution patterns are described as random or blockwise (Daas, Meyer-Hansen, Schols, De Ruiter, & Voragen, 1999; Guillotin et al., 2005; Levesque-Tremblay, Pelloux, Braybrook, & Müller, 2015; Willats, Knox, & Mikkelsen, 2006). Non-esterified GalA distribution patterns were first defined by Daas et al. (Daas et al., 1999) as the degree of blockiness (DB) and absolute degree of blockiness (DB_{abs}) (Daas, Voragen, & Schols, 2000; Guillotin et al., 2005). DB is indicating the relative amount of non-esterified GalA residues present in PG degradable blocks, representing the distribution of non-esterified blocks in relation to the total of non-esterified GalA residues of the pectin molecule, while DB_{abs} is representing the distribution of non-esterified blocks over the entire pectin molecule. Other parameters describing also the methyl-esterified sequences over the backbone are degree of blockiness of methyl-esterified oligomers by PG (DB_{PGme}) and degree of blockiness of methyl-esterified oligomers by PL (DB_{PLme}) (Jermendi, Beukema, van den Berg, de Vos, & Schols, 2021). DB_{abs} shows the fully non-esterified segments of the backbone, while DB_{PGme} and DB_{PLme} illustrate the different methyl-esterified sequences of the pectin degradable by PG or PL.

Sahasrabudhe et al. have shown that TLR2/1 is inhibited by lemon pectins in a DM-dependent manner, where a decreased DM increased TLR2/1 inhibiting and binding properties of pectins Furthermore, it has been observed that not only the level but also the distribution of methyl-esters determines the ability of pectins to influence TLR signaling, the more blockwise methyl-esterified the pectin is, the higher the TLR2/1 inhibitory effect (Beukema, Jermendi, van den Berg, et al.). However, pectins with a similar DM and DB might still have different sequences of non-esterified or methyl-esterified GalA residues (Jermendi, Beukema, van den Berg, de Vos, & Schols, 2021). It is not known whether such different sequences play a role in the interaction between TLR2 and pectins.

The aim of this study was to understand the relationship between pectin structure and conformation and TLR2/1 inhibition. To investigate the structural characteristics of pectins underlying the binding and inhibition of TLR2/1, pectins with known TLR2/1 inhibiting capacities were extensively characterized by enzymatic fingerprinting methods for their level and distribution of methyl-esters. For the binding, molecular relations were measured and simulated in various possible conformations. Now, for the first time, we used docking analysis, which helped to recognize molecular interactions between pectins and TLRs and may be used to understand why only pectins with a certain structure bind to TLRs.

2. Materials and methods

2.1. Materials

Commercially extracted lemon (L) pectins L18 (DM18%), L19 (DM19%), L32 (DM32%), L43 (DM43%), L49 (DM49%) were provided by CP Kelco (Copenhagen, Denmark) and orange (O) pectins O32 (DM32%), O59 (DM59%), O64 (DM64%) were provided by Andre Pectin (Andre Pectin Co. Ltd., Yantai, China). Endo-polygalacturonase (Endo-PG, EC 3.2.1.15) from *Kluyveromyces fragilis* (Daas et al., 1999) and pectin lyase (PL, EC 4.2.2.10) of *Aspergillus niger* (Harmsen, Kusters-van Someren, & Visser, 1990) were used to degrade the citrus pectins. All chemicals were purchased from Sigma Aldrich (St. Louis, MO, USA), VWR International (Radnor, PA, USA), or Merck (Darmstadt, Germany), unless stated otherwise.

2.2. Characterization of pectins

Determination of the neutral monosaccharide composition of citrus pectins was carried out by acid hydrolysis and neutral sugars released were derivatized and analyzed as their alditol acetates (Englyst & Cummings, 1984). Alditol acetates were separated using gas chromatography (GC), equipped with a capillary DB-225 column (0.53 mm diameter, 15 m length, film thickness 1 μm) and flame ionization detector (Focus-GC, Thermo Scientific). The column oven was initially maintained at 180 °C for 2 min after the injection followed by ramping the temperature with 2 °C/min to 210 °C. Helium was used as the carrier gas. Inositol was used as internal standard. Uronic acid content of the hydrolysates was determined by the automated colorimetric *m*-hydroxydiphenyl method as previously described (Blumenkrantz &

Asboe-Hansen, 1973; Jermendi, Beukema, van den Berg, de Vos, & Schols, 2021). To determine the degree of methyl-esterification pectin samples were saponified using 0.1 M NaOH for 24 h (1 h at 4 °C, followed by 23 h at room temperature). The methanol released was measured by a gas chromatography (GC) method as previously described and consequently, the DM was calculated (Huisman, Oosterveld, & Schols, 2004).

2.3. Modification of pectins

O59 and O64 were re-esterified to obtain high methyl-esterified pectins with a rather random methyl-ester distribution by the use of H_2SO_4 in methanol at low temperatures (4 °C) according to the procedure of Heri et al. (Heri, Neukom, & Deuel, 1961) to yield $O85_{O59}$ and $O92_{O64}$ respectively.

Random de-esterification of both $O92_{O64}$ and $O85_{O59}$ was done by saponification with diluted NaOH as described previously (Chen & Mort, 1996) yielding a set of random methyl-esterified pectins ($O55_{RD64}$ and $O56_{RD59}$) with DM values of 55 and 56 %, respectively. The chemical characteristics of the pectin samples are shown in Table A1.

2.4. Enzymatic hydrolysis

All citrus pectins were dissolved in 50 mM sodium acetate buffer pH 5.2 (5 mg/ml). Enzymatic hydrolysis was performed at 40 °C by incubation of the pectin solution with PL for 6 h followed by the addition of endo-PG and incubation for another 18 h (Remoroza, Buchholt, Gruppen, & Schols, 2014). Molecular weight distribution was analyzed by High Performance Size Exclusion chromatography (HPSEC). Released diagnostic oligosaccharides were annotated and quantified using High Performance Anion Exchange Chromatography system with Pulsed Amperometric- and UV-detection (HPAEC-PAD/UV) and by Hydrophilic Interaction Liquid Chromatography (HILIC) with online Electrospray Ionization Ion Trap Mass Spectrometry (ESI-IT-MS) HILIC-ESI-IT-MS.

2.5. HPSEC of native and digested pectins

The molecular weight distribution of all (modified) citrus pectins before and after enzymatic digestion was analyzed using a set of four TSK-Gel super AW columns in series: guard column (6 mm ID × 40 mm) and columns 4000, 3000 and 2500 SuperAW (6 mm × 150 mm) (Tosoh Bioscience, Tokyo, Japan) as described previously (Jermendi, Beukema, van den Berg, de Vos, & Schols, 2021; Voragen, Schols, De Vries, & Pilnik, 1982).

2.6. HPAEC of GalA oligosaccharides

The citrus pectin digests were analyzed and subsequently quantified using a HPAEC-PAD-UV system equipped with a CarboPac PA-1 column as described elsewhere (Broxterman & Schols, 2018; Jermendi, Beukema, van den Berg, de Vos, & Schols, 2021). UV detection was used to identify the unsaturated oligosaccharides. GalA DP 1–3 (Sigma Aldrich, Steinheim, Germany) were used as standards for quantification. Oligomers above GalA DP 3 and unsaturated oligomers were quantified using the response of the GalA DP 3 standard. Higher DP oligomers will be (slightly) underestimated due to decreasing response factors; this approach is widely applied e.g. Van Gool et al. (2013) or Jermendi, Beukema, van den Berg, de Vos, & Schols, 2021.

2.7. HILIC-ESI-IT-MS of methyl-esterified GalA oligosaccharides

Pectin digests were also analyzed using UHPLC in combination with electrospray ionization tandem mass spectrometry (ESI-IT-MS) on a Hydrophilic Interaction Liquid Chromatography (HILIC) BEH amide column. Pectin digests were centrifuged (15,000 ×*g*, 10 min, RT) and diluted with 50 % (v/v) acetonitrile containing 0.1 % formic acid, to a final concentration of 1 mg/ml. A heated ESI-IT ionized the separated oligomers in an LTQ Velos Pro Mass Spectrometer (ESI-IT-MS) coupled to an UHPLC and allowed identification of the methyl-esterified oligomers (Jermendi, Beukema, van den Berg, de Vos, & Schols, 2021). To overcome the limitations of HPAEC due to the elimination of the methyl-esters at high pH (pH 12) (Kravtchenko, Penci, Voragen, & Pilnik, 1993), HILIC-MS was used for the separation and identification of methyl-esterified oligomers (Remoroza et al., 2012). Peaks have been annotated based on the *m/z* of the GalA oligomers, and the relative abundance of selected DPs has been obtained after integration of peak areas in the ion chromatograms (Jermendi, Beukema, van den Berg, de Vos, & Schols, 2021). Following the quantification using HPAEC-PAD, the relative abundance of GalA oligosaccharides obtained from HILIC-MS was applied to differentiate between the differently methyl-esterified and non-esterified oligomers within one DP.

2.8. Calculating descriptive parameters

2.8.1. Absolute degree of blockiness

The absolute degree of blockiness (DB_{abs}) is calculated as the mole amount of GalA residues present in non-methyl-esterified mono-, di- and trimer released by *endo*-PG expressed as the percentage of the total moles of GalA residues present in the pectin (Eq. (1)) (Daas et al., 2000; Guillotin et al., 2005).

$$DB_{abs} = \frac{\sum_{n=1\text{-}3}[\text{saturated GalA}_n\text{released}]_{\text{non-esterified}} \times n}{[\text{total GalA in the polymer}]} \times 100 \quad (1)$$

2.8.2. Degree of blockiness of methyl-esterified oligomers by PG (DB_{PGme})

To describe the partially methyl-esterified HG region of citrus pectins DB_{PGme} was used (Jermendi, Beukema, van den Berg, de Vos, & Schols, 2021). DB_{PGme} is calculated as the number of moles of galacturonic acid residues present in the digest as saturated, methyl-esterified GalA DP 3–8 per 100 moles of the total GalA residues in the pectic polymer (Eq. (2)).

$$DB_{PGme} = \frac{\sum_{n=3\text{-}8}[\text{saturated GalA}_n\text{released}]_{\text{esterified}} \times n}{[\text{total GalA in the polymer}]} \times 100 \quad (2)$$

2.8.3. Degree of blockiness of methyl-esterified oligomers by PL (DB_{PLme})

DB_{PLme} quantifies the amount of unsaturated and methyl-esterified GalA oligomers (DP 2–8) released by the PL. As shown by Eq. (3), all GalA residues present in unsaturated partly methyl-esterified oligomers (DP 2–8), released by PL action were quantified and expressed as degree of blockiness of methyl-esterified oligomers by PL (DB_{PLme}) (Jermendi, Beukema, van den Berg, de Vos, & Schols, 2021).

$$DB_{PLme} = \frac{\sum_{n=2\text{-}8}[\text{unsaturated GalA}_n\text{released}]_{\text{esterified}} \times n}{[\text{total GalA in the polymer}]} \times 100 \quad (3)$$

2.9. TLR2/1 inhibiting assays

The HEK- TLR2-1 inhibition assays were performed as described previously (Beukema, Jermendi, et al., 2020). In short, HEK-Blue hTLR2 were pre-incubated with pectins (2 mg/ml). After 1 h of pre-incubation, cells were stimulated with 10 ng/ml Pam3CSK4 (TLR2-1 agonist), and they were incubated for 24 h. Culture medium was used as negative control and the Pam3CSK4 was used as positive control. Then, cell supernatant was added to Quantiblue (Invivogen) in a ratio of 1:10. After 1 h of incubation, NF-κB activation was quantified at 650 nm using a Versa Max ELISA plate reader (Molecular devices, Sunnyvale, CA, USA). All incubation steps were performed at 37 °C and 5 % CO_2. The percentage of TLR2-1 inhibition by pectins was calculated by comparing NF-κB activation of pectin-treated cells with the positive control. All pectin samples were tested for endotoxins using the endotoxin detection kit (Thermo Scientific, Sunnyvale, CA, USA) and endotoxin levels were below the detection level of 0.1 ng/ml. Each experiment was performed

at least five times.

2.10. In silico molecular docking

To predict the binding site of pectins to TLR2, docking simulation assays were performed. Four HG pectin oligosaccharides of GalA heptamers were chosen as representative compounds. $GalA_7Me^0$, $GalA_7Me^{1,6}$, $GalA_7Me^{1,7}$ and $GalA_7Me^{2,5}$ were defined as ligands. GalA residues were annotated 1–7, counting from the reducing end of the oligosaccharide. $GalA_7Me^{1,7}$ and $GalA_7Me^{2,5}$ 3D structures were constructed and edited using the Optical Structure Recognition Software (OSRA) (Filippov & Nicklaus, 2009). The $GalA_7Me^{1,7}$ structure was used as a framework in Avogadro Molecular Editor (Version 1.2.0) (Hanwell et al., 2012) for construction and energy minimization of the 3D structures of $GalA_7Me^0$ and $GalA_7Me^{1,6}$ (Fig. A3). The experimentally determined crystallographic coordinates of human TLR2-TLR1 heterodimer (PDB code 2Z7X) was used as protein target (Jin et al., 2007). This crystallographic structure was obtained in presence of the synthetic bacterial tripalmitoylated lipopeptide Pam3CysSerLys4 (Pam3CSK4) agonist. Thus, the binding agonist pocket could be included as a potential binding site for the chosen pectins. Energy parameters of the ligands and the target were minimized through the Yasara Energy Minimization Server (Krieger et al., 2009). Molecular docking between TLR2 and pectin oligomers was performed using the protein-small molecule docking web service from the Molecular Modeling Group of the Swiss Institute of Bioinformatics, Lausanne, Switzerland (Grosdidier, Zoete, & Michielin, 2011). After docking simulations, the best energy scored poses were selected and considered as the most likely binding structures. Docking simulations, atomic contacts between target and ligands, and their type of interactions were analyzed with Chimera software (Version 1.14) (Pettersen et al., 2004) and LigPlot+ (Version v.2.2.5) (Laskowski & Swindells, 2011). Figures were prepared with Pymol Molecular Graphics System (Version 2.3.5) Edu, Schrödinger, LLC (DeLano, 2002) and with Chimera software (Version 1.14) (Pettersen et al., 2004).

3. Results and discussion

3.1. Characterization and quantification of pectin diagnostic oligomers

Six pairs of pectins were chosen for their similar DM and their comparable features regarding sugar composition (Table A1) and molecular weight (Mw) distribution (Fig. A1). The selected native pectins have been reported before for their bioactivity (Beukema et al., 2021; Beukema, Jermendi, van den Berg, et al., 2021). In addition, some modified pectins were selected. Two native pectins have been re-esterified and consequently de-esterified close to the DM of the parental pectins. The aim was to discover the bioactivity differences of rather similar pectins with comparable DM, but different methyl-ester distribution patterns. Although, also Mw, type and structure of side chains may affect immune modulation properties of pectin (McKay et al., 2021; Popov & Ovodov, 2013), especially the level- and distribution of methyl-esters will have a strong immunomodulating effect and has been investigated in more detail.

Homogalacturonan degrading enzymes *endo*-PG and PL were used to degrade the pectin backbone and to generate a wide-ranging mixture of diagnostic oligomers. Fig. A1 illustrates that all parental pectins had a rather similar Mw. Only chemical modification caused a minor decrease in the Mw of the modified pectins, although all pectins still had a rather similar Mw. HPSEC further showed clearly that endo-PG and PL together sufficiently degraded pectins. The resulting mixture of diagnostic oligomers was then analyzed by HPAEC and HILIC.

HPAEC-PAD/UV of the endo-PG and PL degradation products of pectins allowed the separation, identification, and quantification of GalA monomers and both saturated and unsaturated oligomers ranging from DP 2–7 (Fig. 1). The diagnostic oligomer profiles obtained from HPAEC suggested that the pectin pairs all released similar oligomers after degradation. However, as a consequence of pH 12 used during the

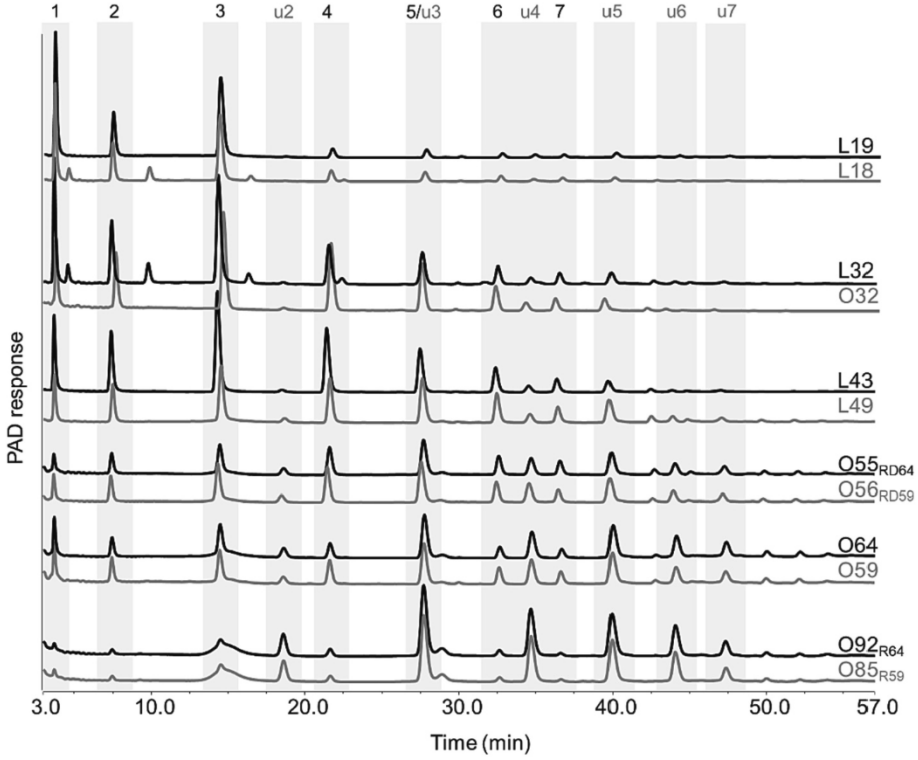

Fig. 1. HPAEC-PAD elution patterns of *endo*-PG and PL digests of pectins after 24 h incubation detected by PAD. Peak annotation: 4, saturated DP4 GalA oligosaccharide; u4, unsaturated DP4 GalA oligosaccharide. Pectin codes: O: orange origin, L: lemon origin, Number: DM. L18 = Lemon pectin with a DM of 18, RD: pectin has been re-esterified and consequently de-esterified using alkali from parental pectin, R: pectin has been re-esterified from parental pectin.

HPAEC analysis, information on the methyl-esterification of the different oligomers was lost, and therefore, it was not possible to distinguish between methyl-esterified and non-esterified oligosaccharides. To counteract this loss of information on methyl-esters, also HILIC-MS was used to separate and identify methyl-esterified oligomers (Jermendi, Beukema, van den Berg, de Vos, & Schols, 2021; Remoroza et al., 2012) and to obtain the relative abundance of selected oligomers after integration of peak areas in the ion chromatograms as described previously (Jermendi, Beukema, van den Berg, de Vos, & Schols, 2021). By combining HPAEC and HILIC-MS data, the methyl-ester distribution patterns of pectins were characterized in detail (Fig. 2).

The diagnostic oligomers as present in different ratios in the HILIC elution patterns of the PG-PL enzyme digests of the twelve citrus pectins, indicated diverse methyl-ester distribution patterns for the rather similar DM pectins (Fig. 2). Besides the non-esterified GalA 2^0 and 3^0, it has been clearly seen that both saturated and unsaturated oligomers with the same DP and different levels of methyl-esterification such as 4^1, 4^2, $u4^2$, $u4^3$ etc., were also nicely separated. However, a complete chromatographic separation of all GalA isomers, i.e., oligomers merely varying in the position of methyl-esters was not attained, but distinction could be obtained by extracted ion chromatograms (Leijdekkers, Sanders, Schols, & Gruppen, 2011).

To visualize the differences in the oligomer profiles of pectins, especially for the similar DM pectins, a bar chart has been created. Fig. 3 clearly shows how much the released oligomers differ in amount for digests from e.g., the pectin pairs. The figure visualizes the relative amounts of the various diagnostic oligomers, as released by PG (saturated, non-esterified mono-, di- and triGalA and methyl-esterified oligosaccharides) and the unsaturated, methyl-esterified oligomers released by PL. As expected, the level of oligomers released by PG decreased with an increase in DM and, at the same time, the amounts of oligomers released by PL were increasing.

The figure is quite revealing in several ways. First, a rather big difference has been observed between pectins L18 and L19, regardless of the 80 % non-esterified GalA residues in the backbone. As expected DP1–3 were the most dominant products but differed slightly in amount. Looking at the yellow and blue segments (Fig. 3), it can be seen that L18 had more methyl-esterified oligomers released by PG, than L19, and the PL degradation products also varied for the two pectins. The PL degradable regions of L32, O32 and even L43 pectins were similarly minor as the very low DM pectins L18/19 PL degradable regions. In the aforementioned pectins, the level of PG degradable completely non-esterified and partially esterified regions however, shifted compared to the L18/19 pectins as expected. Looking at the degradation profiles of the two parental high DM pectins O64 and O59 and the modified $O55_{RD64}$ and $O56_{RD59}$ pectins, it was seen that while the parental pectins

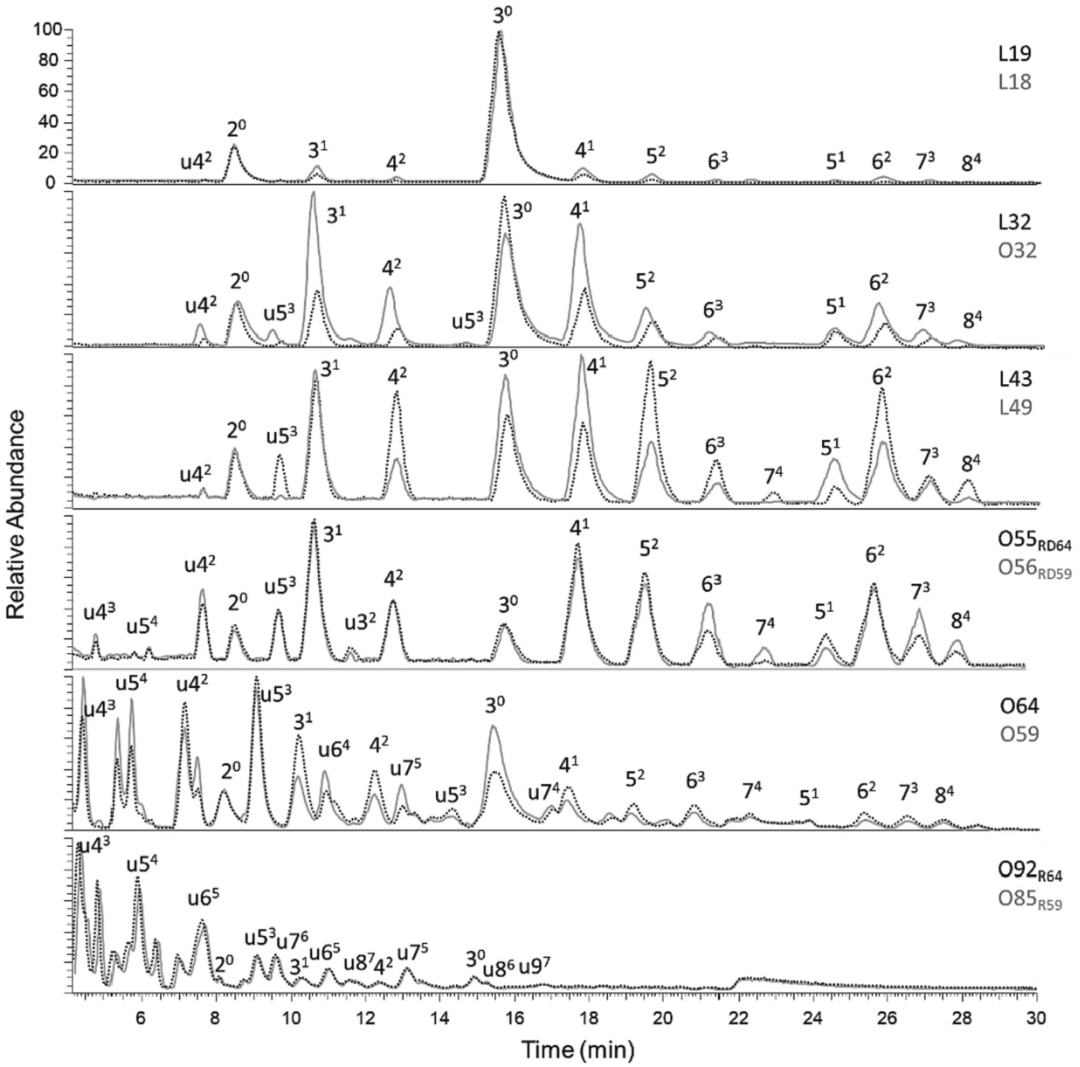

Fig. 2. HILIC-MS base peak elution pattern of pectins digested by the enzymes *endo*-PG and PL. Peak annotation: 3^1, saturated DP3 GalA oligosaccharide having one methyl-ester; $u5^3$, unsaturated DP5 GalA oligosaccharide having three methyl-esters Pectin codes: O: orange origin, L: lemon origin, Number: DM. L18 = Lemon pectin with a DM of 18, RD: re-esterified and consequently alkali de-esterified pectin, R: re-esterified from parental pectin.

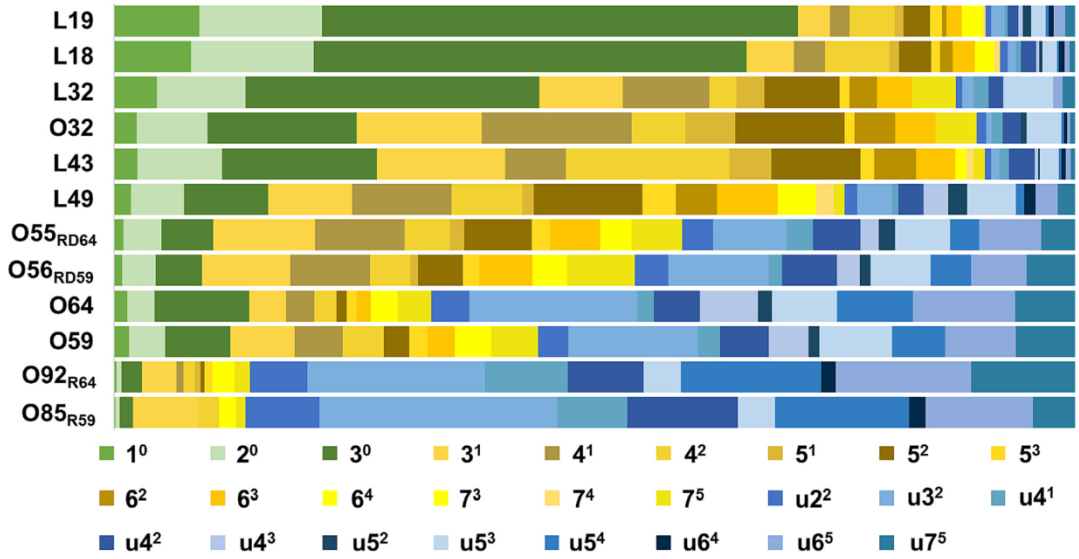

Fig. 3. Relative abundance of released diagnostic oligomers of citrus pectins after incubation with *endo*-PG and PL. Oligosaccharides were quantified using HPAEC-PAD and HILIC-MS. Annotation: $u3^2$, u = unsaturated, 3 = number of galacturonic acid residues, superscript ^{2} = number of methyl-esters present on the GalA residue. L: lemon origin, O: orange origin, Number: DM. L18 = Lemon pectin with a DM of 18, R: re-esterified pectin, RD: re-esterified and consequently alkali de-esterified pectin, green colours represent non-Me GalA oligomers released by PG; yellow colours represent Me GalA oligomers released by PG; and blue colours represent unsaturated Me GalA oligomers released by PL.

had quite different degradation products, after the modification, their profiles became fairly similar. Furthermore, the re-esterified $O92_{R64}$ and $O85_{R59}$ pectins similarly to the very low DM pectins still showed different degradation products upon digestion and as expected, primarily unsaturated PL oligomers dominated.

From Fig. 3, it is apparent that pectins having similar DM values show noticeably different patterns. Prior studies have already noted the importance of characterization of methyl-esterification patterns in pectin (Daas et al., 2000; Guillotin et al., 2005; Ralet et al., 2012). It has been revealed that different techno- and biofunctional properties of rather similar DM pectins could not be explained by the commonly used characteristics. Characterization of pectins in more detail has been proven to be possible and beneficial by e.g., Jermendi, Beukema, van den Berg, de Vos, & Schols, 2021. Using the simultaneous endo-PG and PL digestion and combined HPAEC and HILIC analysis to separate and quantify pectic oligomers released from these citrus pectins helped to realize that similar DM pectins can have different methyl-ester distribution. Regarding bioactivity, Sahasrabudhe et al. (2016) have demonstrated that the DM was responsible for the distinction between pectins, but surprisingly, it was also found that various pectins with the same DM still had different TLR recognition behaviors (Beukema, Jermendi, van den Berg, et al., 2021). Therefore, the difference revealed in the methyl-ester distribution is expected to result in different biological effects on TLR recognition.

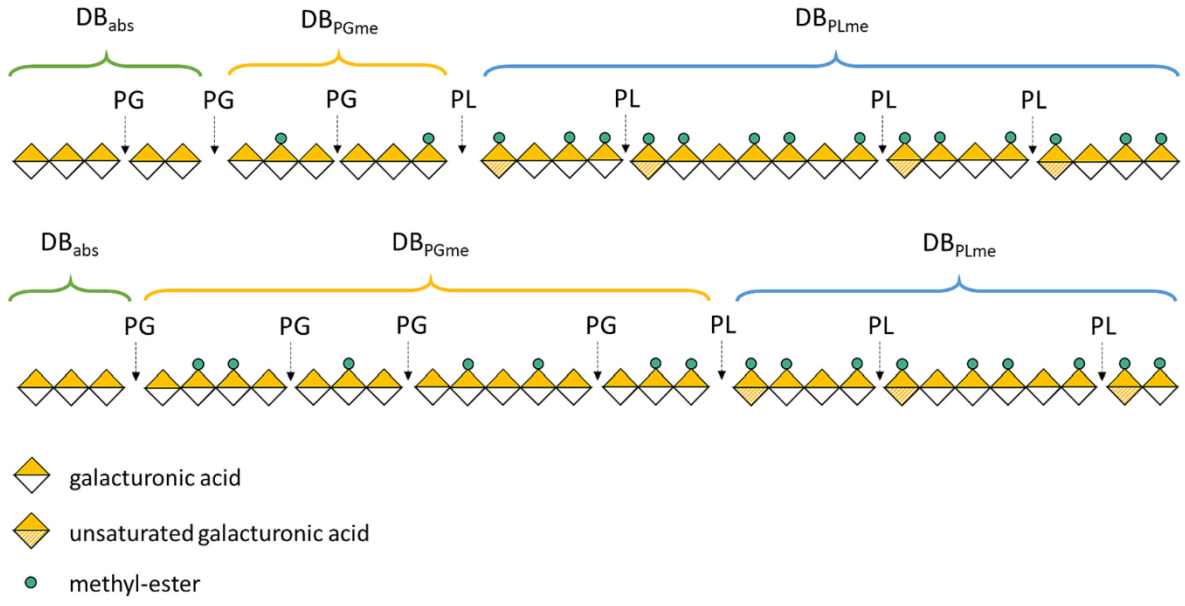

Fig. 4. Schematic representation of a hypothetic backbone of two high DM pectins with different methyl-ester distributions after combined digestion of PG and PL including the descriptive parameters DB_{abs}, DB_{PGme} and DB_{PLme}. The sequence of oligosaccharides is hypothetical.

3.2. Descriptive parameters of pectin

3.2.1. Parameters highlighting structural features of pectin's methyl-esterification

The differences in methyl-ester distribution patterns of citrus pectins can be described by the parameters DB_{abs}, DB_{PGme} and DB_{PLme} (Guillotin et al., 2005; Jermendi, Beukema, van den Berg, de Vos, & Schols, 2021). These parameters were calculated from the amounts of specific oligosaccharides released from the various pectins used in this study. As it was apparent already from Fig. 3 that the quantification of diagnostic oligosaccharides resulted in quite different descriptive parameters. Consequently, these parameters allowed us to identify different methyl-ester distribution patterns of pectin pairs, regardless of their similar DM (Jermendi, Beukema, van den Berg, de Vos, & Schols, 2021). Fig. 4 illustrates in a simplified way that two high DM pectins can have considerable variations especially in the methyl-esterified sections of the backbone. Depending on the position of the methyl-esters, PG and PL have cut the backbone at different positions resulting in different diagnostic oligomers.

A high DB_{abs} indicates a more blockwise distribution of non-esterified GalA residues in the pectin. The methyl-esterified diagnostic oligomers liberated by PG represented by the DB_{PGme} are the less methyl-esterified segments of pectin which still have a pattern of methyl-esterification outside the non-esterified blocks. In addition, DB_{PLme} represents the highly methyl-esterified oligomers released by PL. In DB_{PLme} oligomers the methyl-esters are more closely associated than in the DB_{PGme} oligosaccharides. The differences in DB_{PGme} and DB_{PLme} already suggested more refined structural differences in the pectin pairs. Moreover, the ratio of DB_{PGme}/DB_{abs} has also been introduced, which is the ratio of moderately methyl-esterified GalA oligomers (DB_{PGme}) and the completely non-esterified GalA oligomers (DB_{abs}), both of which are released by PG. The DB_{PGme}/DB_{abs} ratio indicates a distinct distribution pattern of the non-esterified GalA blocks over the backbone.

3.2.2. Methyl-esterification patterns in pectins studied

Table 1 shows the descriptive parameters for the six pectin pairs used in this study. The pectin pairs differ in the distribution of methyl-esters over the pectin's backbone as illustrated by their DB_{abs}, DB_{PLme} and DB_{PGme}. In general, for all six pectin pairs, the DB_{PGme}/DB_{abs} ratio was lower for the higher DB_{abs} pectins of the similar DM pectin pairs.

Table 1
Descriptive parameters and TLR 1/2 inhibition of commercial and modified pectins used in this study.

Sample[a]	DM[b]	DB_{abs}[c]	DB_{PGme}[d]	DB_{PLme}[e]	DB_{PGme}/DB_{abs}	TLR 2/1 inhibition (%)
L19	19	75	21	10	0.3	54
L18	18	66	27	8	0.4	48
L32	32	48	47	14	1.0	51
O32	32	24	60	10	2.5	35
L43	43	32	73	11	2.3	62
L49	49	18	65	26	3.7	45
$O55_{RD64}$	55	10	46	38	4.7	24
$O56_{RD59}$	56	8	38	39	4.9	23
O64	64	14	18	65	1.3	45
O59	59	12	30	53	2.6	28
$O92_{R64}$	92	3	10	75	3.9	30
$O85_{R59}$	85	2	14	99	5.9	17

[a] O: orange origin, L: lemon origin, Number: DM. L18 = Lemon pectin with a DM of 18, RD: pectin has been re-esterified and consequently de-esterified using alkali from source pectin, R: pectin has been re-esterified from source pectin.
[b] Degree of methyl-esterification (DM): mol of methanol per 100 mol of the total GalA in the sample.
[c] Absolute degree of blockiness (DB_{abs}): the amount of non-esterified mono-, di- and triGalA per 100 mol of total GalA in the sample.
[d] Degree of blockiness by *endo*-PG (DB_{PGme}): the amount of saturated methyl-esterified galacturonic residues per 100 mol of total galacturonic acid in the sample.
[e] Degree of blockiness by PL (DB_{PLme}): the amount of methyl-esterified unsaturated galacturonic oligomers per 100 mol of total galacturonic acid in the sample.

3.2.3. DM ~20 pectins

For the very low DM pectins the DB_{abs} was the highest and DB_{PLme} was the lowest of all pectins, just as expected, as 80 % of the backbone was non-esterified and the methyl-esters could not be too closely positionated. Compared to pectin L19, it can be seen that the DB_{abs} and DB_{PLme} for pectin L18 was somewhat lower while the DB_{PGme} was higher, which points out that the methyl-ester distribution differed for the two pectins even though both of them had a very low DM. Looking at the DB_{PGme}/DB_{abs} ratio for L19, it was lower than for L18, but still rather similar (0.3 and 0.4 respectively).

3.2.4. DM ~30 pectins

Between the low DM30 pectins, there were considerably higher differences. L32 and O32 had highly different DB_{abs} and DB_{PGme} values, while their DB_{PLme} values were somewhat similar. The DB_{abs} of O32 pectins was found to be half of L32 (24 and 48 respectively) which suggests a very random distribution of the O32 pectin. The high DB_{PGme} of the O32 pectin supports the low DB_{abs} value, referring to parts of the backbone which are methyl-esterified in such a way that PG was still able to act. The DB_{PLme} of the DM30 pectin pair was fairly similar meaning that also more densely methyl-esterified segments of the backbone were present and in rather comparable amounts. It can thus be suggested that the PL degradable methyl-esterified segments of both of the pectins were fairly similar, while the PG degradable non-esterified segments in L32 pectin were rather long, and in O32 they were interrupted with methyl-esters. The ratio of DB_{PGme}/DB_{abs} was also 2.5 times higher for the O32 pectin, suggesting a random distribution of methyl-esters.

3.2.5. DM ~45 pectins

For the intermediate DM pectins L43 and L49, a fairly different trend was shown since their DB_{abs} and DB_{PLme} values were greatly different while their DB_{PGme} were comparable also to the DM ~ 30 pectins. Suggested by the higher DB_{abs} L43 had longer blocks of non-esterified GalA residues compared to L49. Interestingly the high DB_{PGme} and low DB_{PLme} values propose that the methyl-esterified segments were actually more randomly distributed over the backbone for L43, despite having a higher DB_{abs}. L49 had less blockwise non-esterified GalA distribution. The higher DB_{PLme} for L49 showed that the methyl-esters over the backbone were more closely associated compared to the L43 pectin. This means that L49 pectin had a random distribution in the PG degradable segments, while in the PL degradable segments the methyl-esters were distributed closer together.

3.2.6. DM ~60 pectins

O64 and O59 had comparable DM and DB_{abs} values (14 and 12 respectively). DB_{PLme} was higher for O64 compared to O59 and DB_{PGme} of O64 was almost half of O59. It is believed that O64 pectin, while having somewhat longer non-esterified blocks, also had closely associated methyl-esters distributed over the backbone, compared to the more random O59. The ratio of DB_{PGme}/DB_{abs} was also much lower in O64 pectin compared to O59 (1.3 and 2.6 respectively), further supporting the different methyl-ester distributions. The structural differences between the two commercial pectins were striking, as they were produced by the same company, extracted from the same raw material and had similar DM.

3.2.7. Re-esterified, DM ~90 pectins

The very high DM pectins $O85_{R59}$ and $O92_{R64}$ have fairly low chances of having blocks of non-esterified GalA sequences, which is also shown by their rather low DB_{abs} (2 and 3 respectively). The very high DM is recognised as well by the very high values for DB_{PLme} (75 and 99

respectively). Yet surprisingly $O85_{R59}$ and $O92_{R64}$ pectins still had their own, slightly different, methyl ester distributions over their backbone as shown by their DB_{PGme} (14 and 10 respectively) and the ratio of DB_{PGme}/DB_{abs} (5.9 and 3.9 respectively). The aim of re-esterification was to create two similar, fully esterified pectins, however, they both kept some of the properties of their parental pectins. Unlike what has been suggested by Daas et al. (Daas et al., 1999) and others, re-esterification of pectins to DM > 90 is not sufficient to obtain a fully randomly methyl-esterified pectin.

3.2.8. De-esterified, DM ~55 pectins

The re-esterification and consequent de-esterification of the blocky O64 pectin resulted in a highly random pectin $O55_{RD64}$, which can be seen also from the lower DB_{abs} and a substantial increase in DB_{PGme}/DB_{abs} ratio compared to the parental pectin. The DB_{PGme}/DB_{abs} ratio was among the highest for the two randomized pectins, $O55_{RD64}$ and $O56_{RD59}$ (4.7 and 4.9 respectively). In general, the two de-esterified pectins became fully random compared to the parental pectins but $O55_{RD64}$ was found to be more blockwisely distributed, just as its parental O64 pectin.

The data indicated by the DB_{PGme}/DB_{abs} ratio obtained after combined PG and PL digestion of pectins can be probably best explained by the parental and modified pectins. As expected, the DB_{PGme}/DB_{abs} ratio was the lowest for pectins releasing higher amounts of non-esterified GalAs and lower methyl-esterified oligomers. For the randomized pectins $O55_{RD64}$ and $O56_{RD59}$ the value of DB_{PGme} increases and DB_{PLme} decreases compared to the parental pectins, which indicated a random pattern of methyl-ester distribution. This suggests that the arrangement of the methyl-esters over the backbone allowed more PG action and the release of saturated non-esterified mono-, di- and tri-GalA and also various methyl-esterified oligomers, and decreased the chances of PL to act as the methyl-esters are less closely associated on the homogalacturonan. As a result, a randomly methyl-esterified pectin would have an increased ratio of DB_{PGme}/DB_{abs}. Although, the two randomized pectins became more similar, the methyl-esters were not equally distributed, despite the same treatment and similar DM.

3.3. Methyl-ester distribution patterns of citrus pectins drive TLR2/1 inhibition

It has been found that citrus pectins can influence immunity through Toll-like receptor (TLR) signaling (Beukema, Jermendi, van den Berg, et al., 2021; Vogt et al., 2016). TLR2-TLR1 dimerization is specifically activated by a Pam3CSK4 agonist and the dimerization induced proinflammatory pathways, therefore inhibiting the TLR2/1 dimerization using pectins can potentially prevent inflammation (Beukema, Jermendi, Koster, et al., 2021; Sahasrabudhe et al., 2016; Sahasrabudhe et al., 2018). The inhibition of TLR2/1 was studied by using the Pam3CSK4 agonist. The TLR2/1 inhibiting capacities of the set of pectins can be seen in Table 1.

Low DM pectins L18, L19 having both low and high DB values all strongly inhibited TLR2/1. L32 pectin with a high DB has shown just as strong inhibition as the L18/19 pectins, while O32 with a low DB inhibited TLR2/1 31 % less than the same DM L32 pectin with a high DB. Intermediate DM pectin L49 with a low DB inhibited similarly to the low DM pectins, and surprisingly L43 with a high DB inhibited about 20 % stronger than the low DM pectins. Among the high DM pectins, O64 having a high DB has shown the strongest inhibition, while the other high DM pectins did not inhibit TLR2/1 as strongly.

Previously it was shown that the impact of citrus pectins on TLRs depends on the DM (Sahasrabudhe et al., 2018; Vogt et al., 2016). A strong relationship between the methyl-ester distribution parameter DB and the TLR2/1 inhibition has been reported by Beukema et al. (Beukema, Jermendi, van den Berg, et al., 2021), suggesting that methyl-ester distribution patterns of pectins play a role in TLR2/1 binding. The presence of distinct blocks of non-methyl-esterification is more important for a good binding and inhibition than the overall charge of the pectin as determined by the DM. However, both DM and DB could not fully explain the inhibition for all pectins as published before (Beukema, Jermendi, Koster, et al., 2021; Beukema, Jermendi, van den Berg, et al., 2021). Therefore more pectins were chosen in this study, including methyl-ester-distribution modified pectins and the TLR2/1 inhibition were measured for all pectins.

In search of the descriptive parameter that would explain the level of TLR2/1 inhibition, it was found that the ratio of DB_{PGme} to DB_{abs} showed the highest correlation to the TLR2/1 inhibition. DB_{PLme} has been shown not to contribute to the correlation (results not shown). It is striking from Fig. 5, that for example, O64 pectin with a (low) DB_{PGme}/DB_{abs} ratio of 1.3 inhibits TLR2/1 stronger than lower DM pectins and higher DB pectins. Since the DB_{abs} is not correlating similarly as the DB_{Pgme}/DB_{abs} ratio, it is clear that not only a long stretch of non-methyl-esterified GalA residues is necessary for optimal binding.

The L18 and L19 pectins both belong to the most strongly TLR2/1 inhibiting pectins, as already claimed before for LM pectins (Sahasrabudhe et al., 2018). Our hypothesis that there is a certain pattern of methyl-esterification needed for TLR2 binding is underpinned by the finding that DM0 pectin (polygalacturonic acid) bound to TLR2 less than low DM pectins (Sahasrabudhe, Tian, et al., 2016). Our results suggest that most probably, next to a non-esterified GalA segment, also a PG degradable segment with a specific methyl-ester distribution is important for binding to TLR2. O32 and L49 were found to inhibit TLR2/1 less than L32 and L43, which corroborates the findings that the TLR2 binding cannot be exclusively explained by the DM or DB (Fig. A2). It is also important to note that DB_{abs} does not offer information on the size of non-esterified blocks (Daas, Voragen, & Schols, 2001; Guillotin et al., 2005). The non-esterified block sequence in pectins with a remarkably high DM, such as $O92_{R64}$ and $O85_{R59}$ and in the successfully randomized $O55_{RD64}$ and $O56_{RD59}$ pectins, is probably too short to induce TLR2/1 inhibition. The patterns as indicated by the DB_{PGme}/DB_{abs} ratio in high and intermediate pectins such as O64, L43 and the low DM pectins L19, L18 and L32 pectins are highly inhibitory for TLR2-TLR1 dimerization. An explanation for these differences might be that the combination of non-esterified block size and distribution of methyl-esters both play a role in the TLR2/1 inhibition by pectins as also indicated by the DB_{PGme}/DB_{abs} ratio.

These results provide further support for the hypothesis that pectin inhibits TLR2/1 dimerization by binding to amino acids on the TLR2 binding sites by presumed electrostatic interactions (Sahasrabudhe et al., 2018; Sahasrabudhe, Tian, et al., 2016). High DB_{abs} pectins have many negatively charged GalA in sequence, which can possibly interact with the TLR2 ectodomain (Hu et al., 2021). Even though the number of non-methyl-esterified GalA and consequently the non-esterified blocks in low DM pectins is certainly more than in high DM pectins, there is a given pattern of methyl-esterified GalAs needed for the inhibitory effect.

3.4. Pectins interact with different TLR2 sites in a pattern-dependent fashion

In our study, pectins with a certain block size of non-esterified GalA residues next to sequences of methyl-esterified GalA residues had a stronger inhibitory effect on TLR2. Molecular docking analysis was performed to gain insight into the molecular mechanisms that drive this inhibitory effect of pectins on TLR2 and to validate our hypothesis that a specific distribution or pattern of methyl-esters plays an important role. To foresee whether there is a specific methyl-ester distribution pattern over the GalA backbone of pectins that binds stronger to TLR2, a non-methyl-esterified heptamer of GalA and three heptamers of GalA residues that differed in methyl-ester distribution were modelled for their best fit to interact with the human TLR2 (PDB code 2Z7X). One heptamer without methyl-esters was used to represent the longest block of GalA residues ($GalA_7Me^0$). Another heptamer contained methyl-esters at GalA residues #1 and #7 (counting from the reducing end)

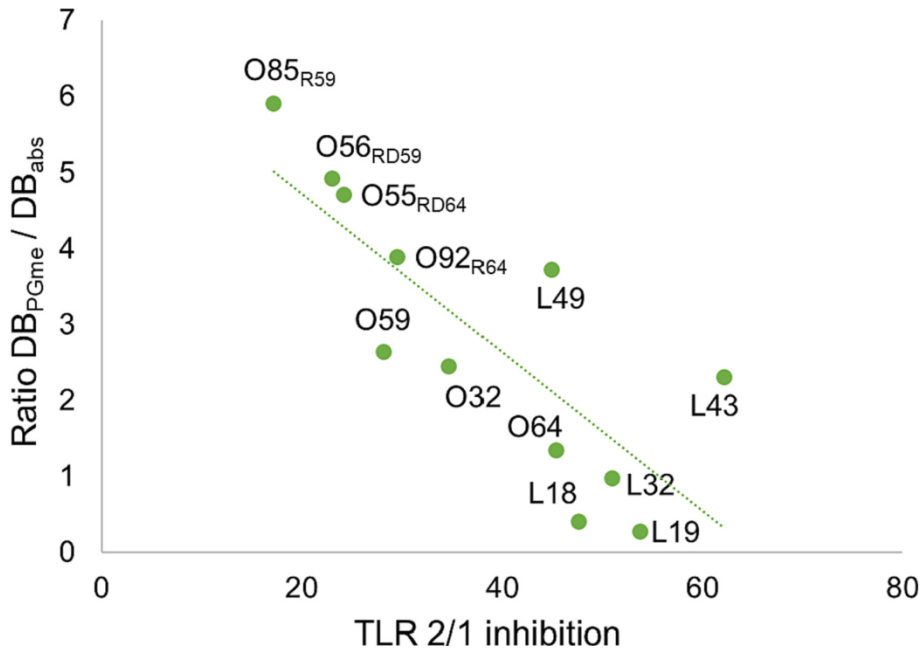

Fig. 5. Ratio of TLR2/1 inhibition plotted versus the DB_{PGme}: DB_{abs} of pectin digests. $R^2 = 0.64$. Negative correlation is shown between the TLR2/1 inhibition and the DB_{PGme}: DB_{abs} ratio. DB_{PGme}: DB_{abs} is the ratio of all methyl-esterified saturated oligos to the non-esterified saturated oligos degraded by PG. Inhibition of TLR2/1 by citrus pectins. HEK-Blue™ hTLR cells were first pre-incubated for 1 h with pectins (2 mg/ml) and subsequently stimulated with the Pam3CSK4 agonist.

($GalA_7Me^{1,7}$), which leads to a sequence of 5 non-esterified GalA residues and one heptamer contained methyl-esters at GalA residues #1 and #6 ($GalA_7Me^{1,6}$), which lead to a short sequence of 4 non-esterified GalA residues. Finally, a heptamer contained methyl-esterified GalA residues at positions #2 and #5 ($GalA_7Me^{2,5}$), representing a sequence of only 2 non-esterified GalA residues (Fig. A3).

The best-ranked pose of $GalA_7Me^0$ had a binding affinity (ΔG) prediction to TLR2 of −12.87 kcal/mol and was located within the agonist binding pocket of TLR2 (Fig. 6A). Molecular docking analysis showed the interaction of $GalA_7Me^0$ with the N274, N305, P306, F325, N327, S346, F349, and L350 amino acid residues of the agonist binding pocket through nine hydrogen bonds (Fig. 6B). From these, F325, F349, and L350 are key amino acid residues of the binding site.

The best-ranked pose of $GalA_7Me^{1,7}$ had a binding affinity prediction to TLR2 of −10.94 kcal/mol, which was located at the heterodimer TLR2/1 interface (Fig. 7A-B). Key amino acid residues from TLR2 which participate in the TLR2/1 interface made contact with $GalA_7Me^{1,7}$: amino acid residues E369 N345 and H398 interacted through hydrogen bonds, and K347 made contact by electrostatic interactions (Fig. 7C). The *O*-methyl group at GalA #1 was found to interact with Glu residue #369, while methyl substitution at GalA #7 did not make any contact with TLR2 (Fig. 7C).

The best-ranked pose of $GalA_7Me^{1,6}$ had a binding affinity prediction to TLR2 of −11.25 kcal/mol and was located on the central domain of TLR2 (Fig. 8A). Molecular docking analysis shows the interaction of $GalA_7Me^{1,6}$ with the E241, E246, and N274 amino acid residues of the leucine-reach repeats (LRRs) 8–9 at the central domain of TLR2 through seven hydrogen bonds (Fig. 8B). R337, which is part of the carboxyl end domain of TLR2, also interacts with this esterified GalA heptamer by two hydrogen bonds (Fig. 8B). None of the interacting amino acids is important neither for ligand binding of TLR2 nor for dimerization with TLR1. Neither the methyl group at position 1 nor that at position 2 established interaction with TLR2 amino acids.

For $GalA_7Me^{2,5}$, the best-ranked pose had a less favorable binding energy value of −3.43 kcal/mol. $GalA_7Me^{2,5}$was found on TLR2 central domain (Fig. 9A), contacting amino acid residues of the LRRs 7–10 through hydrogen bonds (Fig. 9B). None of the two methyl-esters from $GalA_7Me^{2,5}$ interacted with TLR2 (Fig. 9B).

Together these results show that the heptamer representing a longer non-esterified block ($GalA_7Me^0$), is more efficient in binding to TLR2 interface than the pectin heptamer representing a block of only 2 non-esterified GalA residues ($GalA_7Me^{2,5}$), which may be explanatory for the strong TLR2/1 inhibiting properties of pectins with higher degree of blockiness. Our docking study demonstrated that the longer the block of non-esterified GalA sequence the better the binding to TLR2 at the heterodimer interface. This refines our previous finding about the capacity of pectin to bind to TLR2 (Sahasrabudhe et al., 2018). It is known that the activation and further signaling of TLR2/1 is induced by the binding of the agonist at the central domain of the complex. The agonist binding plays a key role in the approximation of TLR2 and TLR1 and the consequent formation of the TLR2/1 heterodimer-agonist complex. When TLR2 and TLR1 get sufficiently close to each other by the binding of the agonist, other amino acid residues located below the agonist-binding site participate in the formation of this TLR2/1 interface further stabilizing the complex (Jin et al., 2007). Strikingly, the longest block of non-esterified GalA was found buried into the TLR2 agonist binding pocket supporting a block of non-esterified GalA present in pectin the stronger might be their TLR2/1 inhibitory capacity. Obviously, the non-binding part of the relatively large pectin molecule will also contribute to the inhibitory capacity through steric hindering. Herein we also demonstrate in more detail that this binding of pectin at the TLR2/1 interface site prevents the stabilization of the TLR2/1 complex, which reinforces the explanation of the inhibitory effect observed. Previously it has been shown that inhibition of TLR2 by food components can attenuate inflammatory responses (Kiewiet et al., 2018).

3.4.1. *Pectic oligosaccharides vs polysaccharides*

Based on the docking studies using oligomers and the TLR2/1 inhibition of the twelve polymeric pectins, it can be concluded that pectin conformation also plays a role in the binding to the TLR2. Depending on the pattern of methyl-esterification, the intramolecular and intermolecular interactions and three-dimensional conformation of pectins in solution vary (Daas et al., 1999; Renard & Jarvis, 1999). Pectin can form a gel when calcium is present and for that a block of at least 8–12 consecutive non-esterified GalA residues is needed (Voragen et al.,

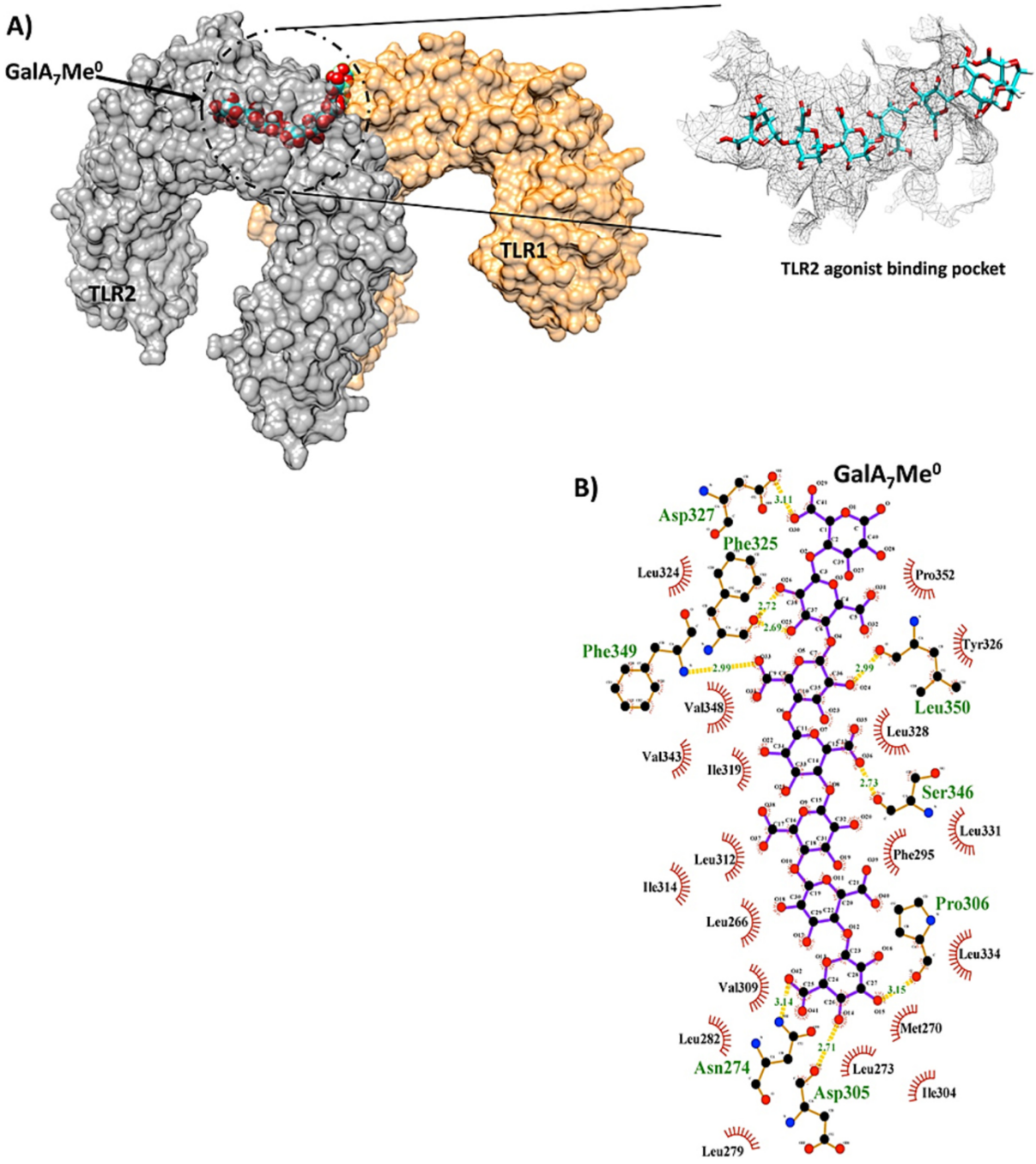

Fig. 6. Binding mode prediction of $GalA_7Me^0$ to TLR2-TLR1 heterodimer by docking simulation. A). Predicted interaction of $GalA_7Me^0$ and hTLR2-TLR1 heterodimer where the non-esterified GalA heptamer fulfils the needed characteristics to be located within the binding pocket of TLR2. The target protein is represented in surface (left) or mesh (right). The pectin ligand is represented in spheres (left) or sticks (right). B). LigPlot diagram of the protein-ligand interactions including hydrogen bonds (dotted yellow lines).

1995). L19, L18, L32, L43, L49 and O64 are the most capable pectins to prevent binding of the TLR2 ligands and by that, inhibit TLR2/1 dimerization. At least 5–7 non-esterified GalA residues need to be available to be able to bind to TLR2, although efficient binding of the segment strongly depends on the three-dimensional conformation of the entire pectic polymer and the number of such binding sites present. Vogt et al. (2016) have shown that pectic oligomers did not activate TLRs. When TLR2 has a pectic polymer bound to it, the size of the polymer may prevent the binding of the agonist even to a different binding site and by that inhibiting the dimerization with TLR1 (Beukema, Jermendi, van den Berg, et al., 2021).

Not only the blockwise distribution of non-esterified GalA residues is important for TLR2/1 inhibition which can be confirmed by the finding that low DM, intermediate DM, and even high DM pectin with a relatively low ratio of DB_{PGme}/DB_{abs} inhibited TLR2/1 dimerization. This finding suggests that a certain non-esterified block size between (partially methyl-esterified GalA residues is important for the ability of pectins to bind to TLR2 and with that to prevent TLR1 to dimerize. The modeling clearly demonstrated that a sequence of 5 non-esterified GalA is more potent for inhibition than a sequence of 2 non-esterified GalA residues for binding to TLR2. More or too many suitable patches within a large pectin molecule might not increase the inhibition due to steric

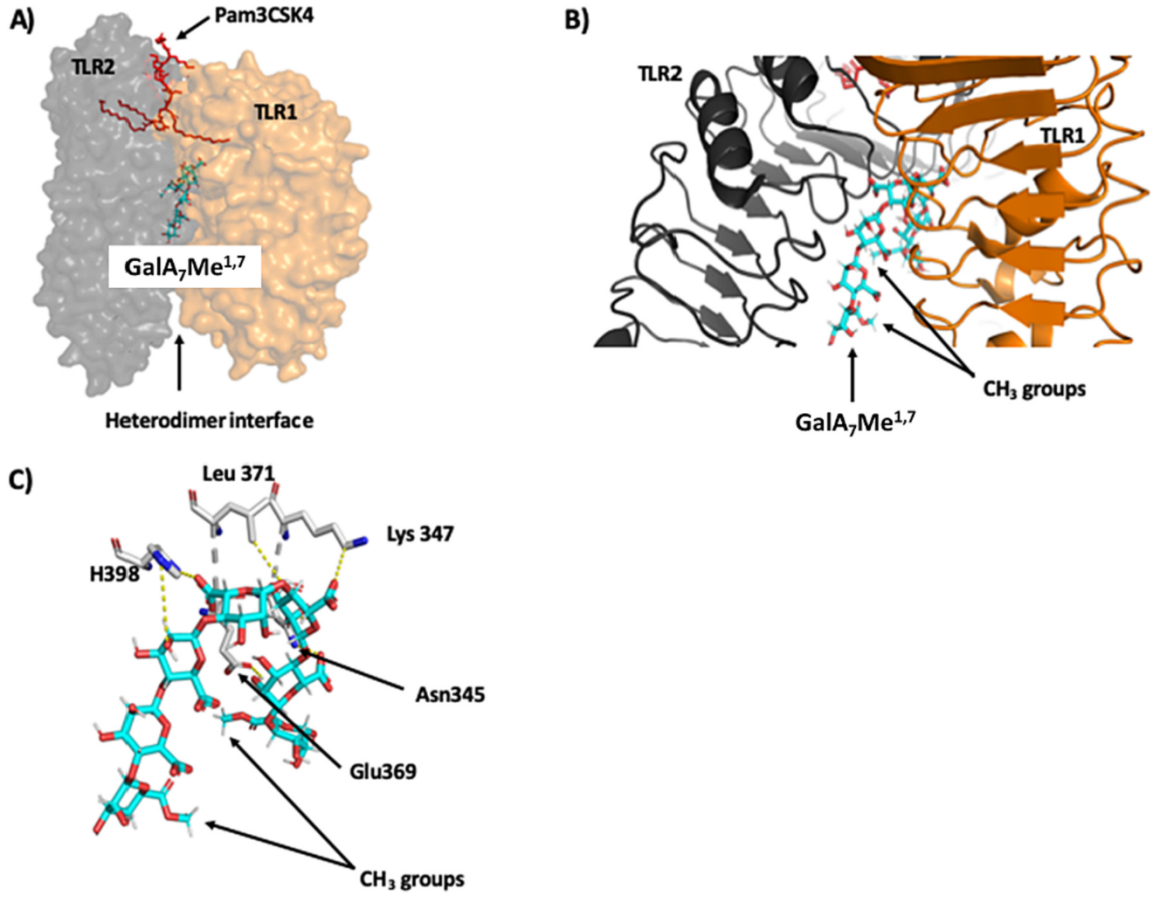

Fig. 7. Binding mode prediction of $GalA_7Me^{1,7}$ to hTLR2-TLR1 heterodimer by docking simulation. A). Overview of hTLR2-TLR1 heterodimer and $GalA_7Me^{1,7}$ interaction. The target protein is represented in surface. The pectin ligand is represented as sticks. TLR2 agonist Pam3CSK4 is depicted in red. B). Close up to the $GalA_7Me^{1,7}$ predicted interaction site, the protein is represented in cartoon. C). Interface TLR2 amino acid residues interacting with $GalA_7Me^{1,7}$ are represented in sticks and yellow dotted lines indicate atomic contacts.

hindrance. The optimal stretches of non-esterified GalAs, and the methyl-esterification patterns together make the non-esterified blocks not too long, but also not too short. The outcomes of the docking analysis are highly valuable, although these findings are somewhat limited by the fact that only two heptamers of GalA residues were used for the docking analysis. More modeling would be needed to reveal more insights on the binding of the homogalacturonan to the TLR2.

By modulating TLR signaling and improving the intestinal immune barrier function, pectin may protect against chronic inflammatory diseases such as Crohn's disease or ulcerative colitis adding to pectin's therapeutic potential (Shibata et al., 2014). In the future it would be useful to perform biological studies with immune cells expressing TLR2 to study the effect of pectins on further signaling, such as production of cytokines, antioxidant enzymes and other molecules under normal and LPS-simulated conditions or other sterile infection with inflammatory molecules. Apart from that, it would be important to compare the use of commercial pectins with that of herbal native pectins rich in arabinogalactan structures to modulate the immune system. Although more detailed studies are needed, our findings certainly add to the understanding of the beneficial immunomodulatory effects of pectins, which may be explained by their impact on TLR2 and decrease of proinflammatory responses. The findings reported here shed new light on the fact that the methyl-esterification pattern of a citrus pectin is a highly valuable structural and functional feature and can determine the TLR2 binding capacity of the pectin.

4. Conclusion

The main goal of the current study was to determine the structure-function relationship between pectins and TLR2/1 inhibition. To better understand the underlying mechanisms involved in pectin-TLR2 binding, the relationship between pectin methyl-ester distribution patterns and conformation, and the inhibition of TLR2/1 dimerization was studied. Pectins were extensively characterized using enzymatic fingerprinting methods and the descriptive parameters. DB_{PGme} and DB_{PLme} have been demonstrated to be extremely powerful to differentiate between major and minor differences in the methyl-ester distribution of pectins. It also has been shown that pectins with rather equal DM and even equal DB_{abs} values are quite different in structure and also their behavior is different. Depending on the application, such small differences can be relevant. The detailed structural analysis of 6 pairs of pectins having similar DM, but different DB demonstrated that interactions with TLR2 are occurring in a structure-dependent way. A blockwise pattern of methyl-esterification is needed for the strongest inhibition. It has been also demonstrated that the ratio of partially methyl-esterified to non-esterified oligomers released by PG (DB_{PGme}/DB_{abs}) does point to the patterns of methyl-esterification.

Docking simulations were performed, and the molecular relations between pectin and TLR2/1 were measured using four GalA heptamers being completely non-esterified or having methyl-esters on different positions to represent methyl-esterification patterns. It was established that at least 5–7 non-esterified GalA residues are necessary next to each other for the binding to TLR2. However, the binding of the GalA segment may strongly depend on the conformation of the pectic polymer and the

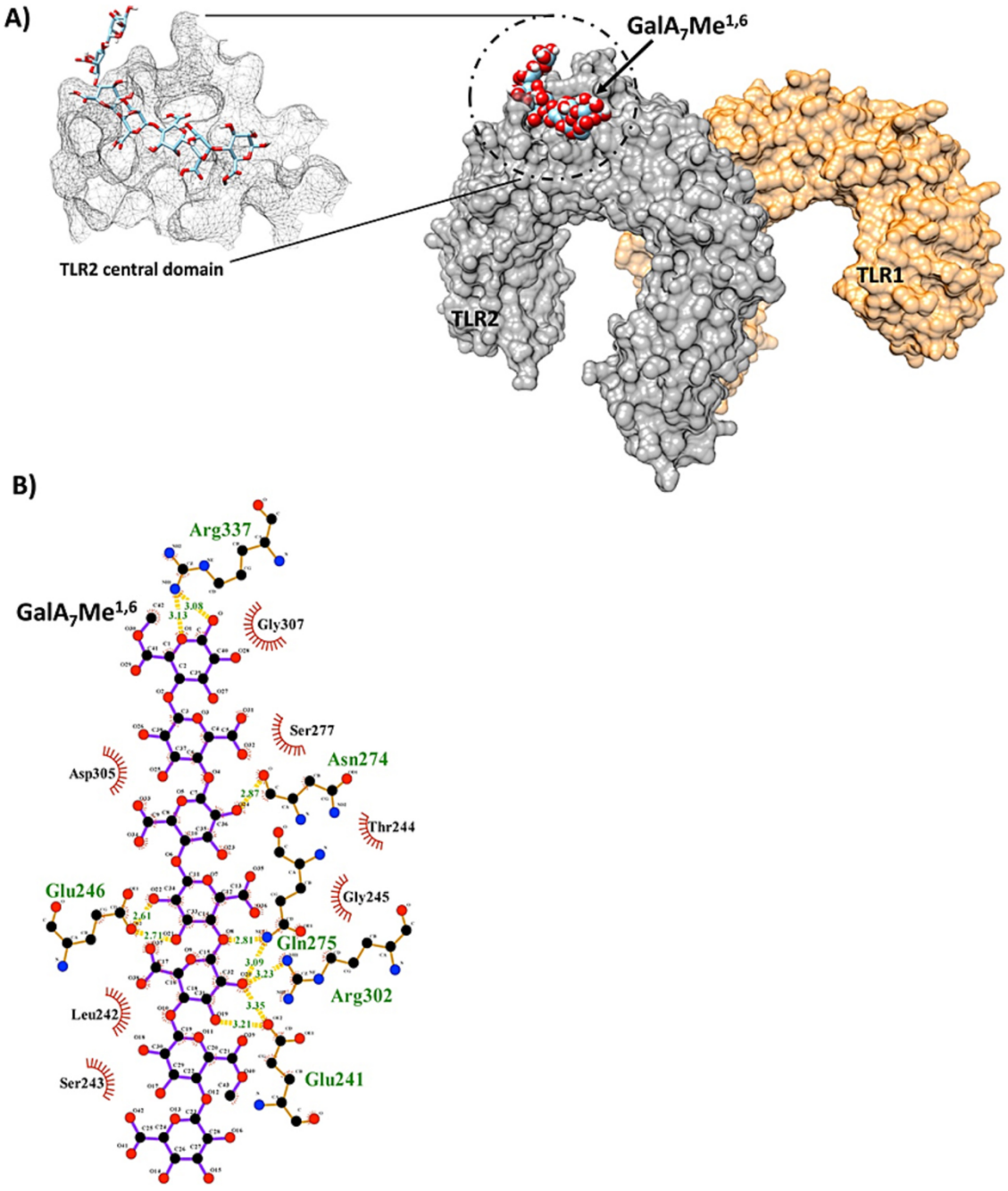

Fig. 8. Binding mode prediction of $GalA_7Me^{1,6}$ to hTLR2-TLR1 heterodimer by docking simulation. A) Predicted interaction of $GalA_7Me^{1,6}$ and hTLR2-TLR1 heterodimer where the esterified GalA heptamer locates on the central domain of TLR2. The target protein is represented in surface (right) or mesh (left). The pectin ligand is represented in spheres (right) or sticks (left). B). Ligplot diagram of the protein-ligand interactions including hydrogen bonds (dotted yellow lines).

number of available binding sites. These results further corroborate the understanding of the molecular interactions between pectins and TLRs. This knowledge may be used in the future to tailor pectins for the prevention of inflammation.

CRediT authorship contribution statement

Éva Jermendi: Conceptualization, Methodology, Data curation, Investigation, Visualization, Writing – original draft. **Cynthia Fernández-Lainez:** Conceptualization, Investigation, Visualization, Writing – review & editing. **Martin Beukema:** Conceptualization, Methodology, Investigation, Writing – review & editing. **Gabriel López-Velázquez:** Visualization, Writing – review & editing. **Marco A. van den Berg:** Writing – review & editing. **Paul de Vos:** Funding acquisition, Conceptualization, Writing – review & editing. **Henk A. Schols:** Supervision, Funding acquisition, Conceptualization, Validation, Writing – review & editing.

Declaration of competing interest

The authors declare that they have no known competing financial interests or personal relationships that could have appeared to influence the work reported in this paper.

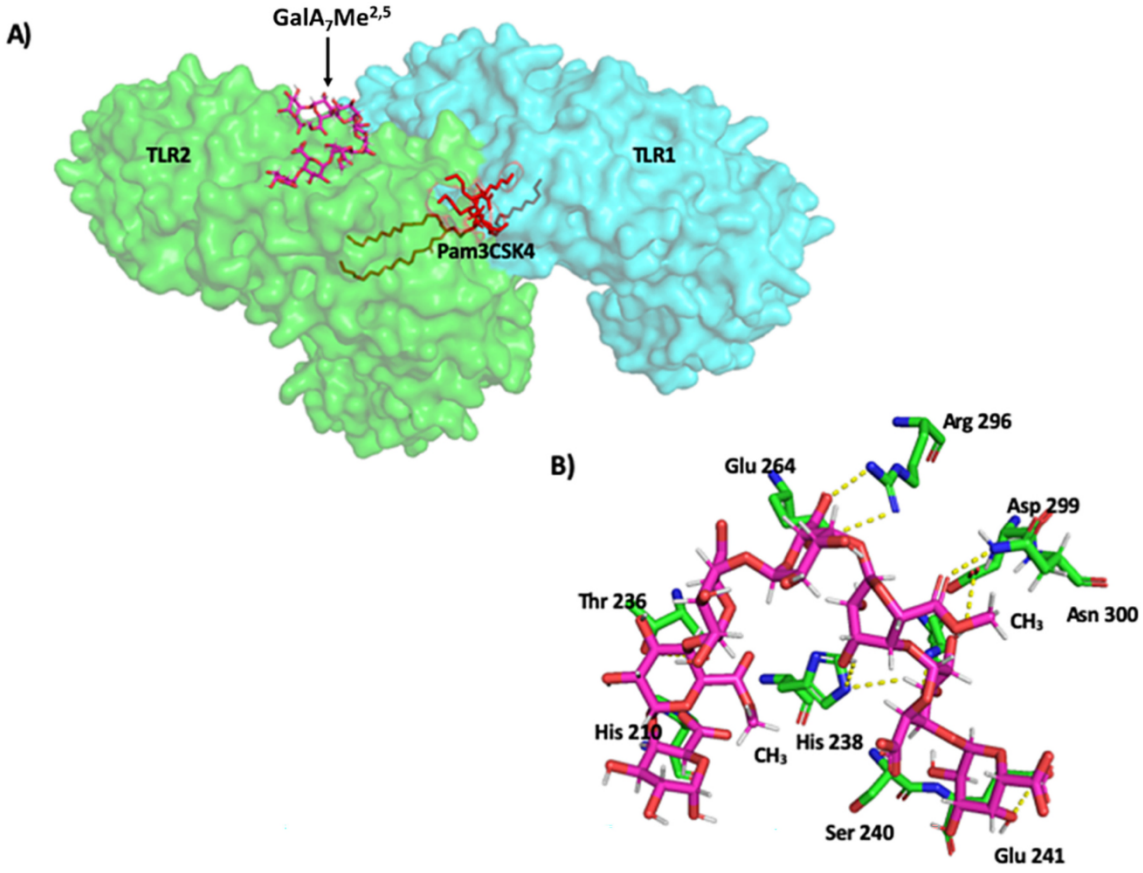

Fig. 9. Docking simulation for interaction site prediction of $GalA_7Me^{2,5}$ with hTLR2-TLR1 heterodimer. Target protein and ligand are represented in surface and sticks, respectively. A). Top overview of the predicted binding mode of $GalA_7Me^{2,5}$ to hTLR2. B) Detailed interaction of $GalA_7Me^{2,5}$ with amino acid residues of the TLR2 central domain, dotted lines indicate atomic contacts.

Data availability

Data will be made available on request.

Acknowledgements

This research was performed within the public-private partnership 'CarboKinetics' coordinated by the Carbohydrate Competence Center (CCC, www.cccresearch.nl). This research is financed by participating industrial partners Agrifirm Innovation Center B.V., Nutrition Sciences N.V., Cooperatie Avebe U.A., DSM Food Specialties B.V., VanDrie Holding N.V. and Sensus B.V., and allowances of The Dutch Research Council (NWO).

Appendix A

Table A1
Characteristics of citrus pectin samples used in this study.

Pectin [a]	Rha	Ara	Gal	Glc	GalA[b]	Total[c]	Mw[d]
	(mol%)					(w/w%)	(kDa)
L19	1.2	1.4	14.1	1.1	81	65	75
L18	0.9	0.6	9.9	0.8	88	63	78
L32	0.9	0.5	7.2	0.5	91	69	70
O32	1.0	3.0	6.0	1.0	89	87	77
L43	0.7	0.3	2.7	0.5	96	64	79
L49	0.8	3.4	6.2	0.6	89	70	114
O64	0.0	7.0	7.0	1.0	84	86	92
O59	1.0	3.0	9.0	3.0	84	83	87
$O92_{R64}$	0.0	0.0	7.0	1.0	91	74	62
$O85_{R59}$	1.0	0.0	8.0	2.0	89	84	55
$O55_{RD64}$	1.0	0.0	8.0	2.0	89	73	60
$O56_{RD59}$	0.0	0.0	9.0	3.0	88	71	54

[a] L: lemon origin; O: orange origin; Number: DM; L19 = Lemon pectin with a DM of 19, RD: pectin has been re-esterified and consequently de-esterified using alkali from source pectin, R: pectin has been re-esterified from source pectin.
[b] Rha = rhamnose, Ara = arabinose, Gal = Galactose, Glc = Glucose, GalA = Galacturonic acid.
[c] Total sugar content in w/w%.

[d] Molecular weight (Mw) in kDa as measured by HPSEC.

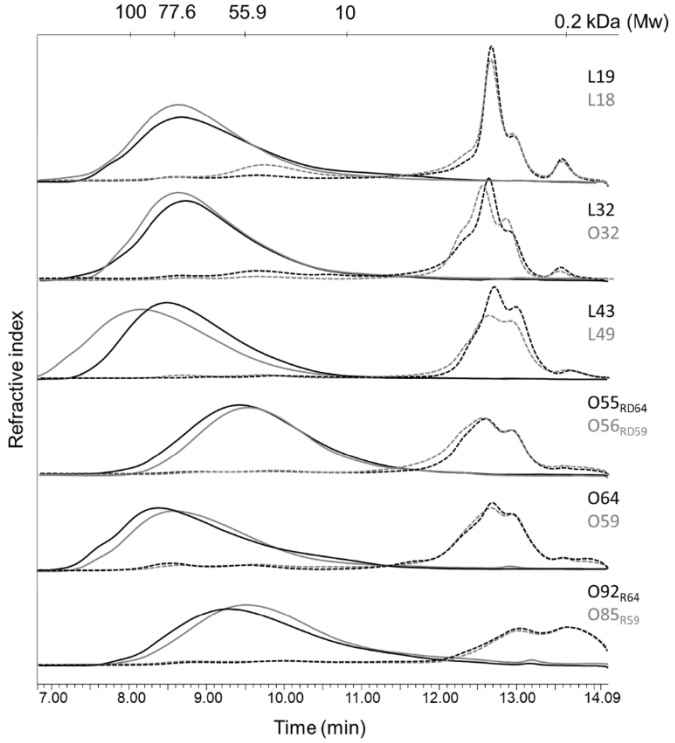

Fig. A1. HPSEC elution profiles of pectins before (solid line) and after (dashed line) digestion by homogalacturonan degrading enzymes: PL and *endo*-PG. Molecular weights of pectin standards (in kDa) are indicated.

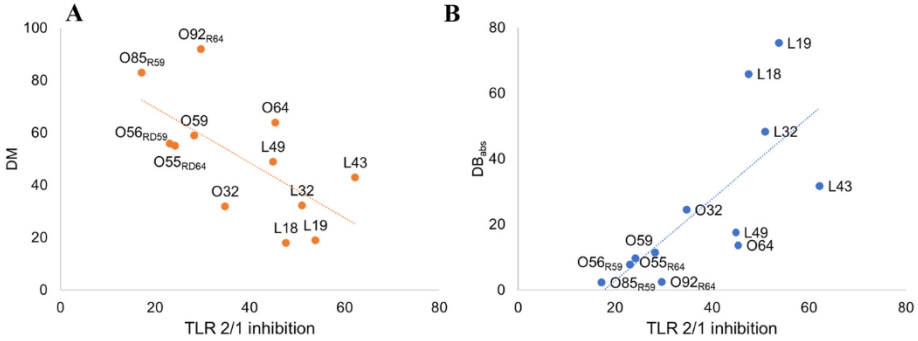

Fig. A2. A) Ratio of TLR2/1 inhibition plotted versus the DB_{abs} of pectin digests. $R^2 = 0.42$
B) Ratio of TLR2/1 inhibition plotted versus the DM of pectin digests. $R^2 = 0.52$.

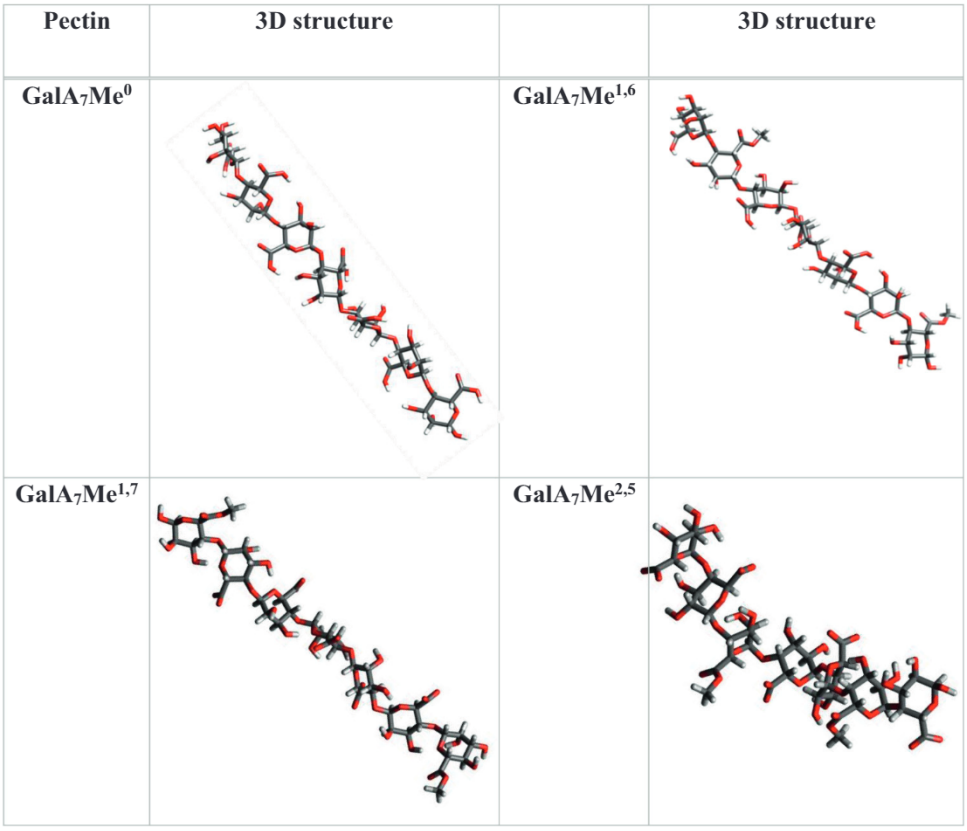

Fig. A3. 3D structures of $GalA_7Me^0$, $GalA_7Me^{1,6}$, $GalA_7Me^{1,7}$ and $GalA_7Me^{2,5}$ GalA heptamers used for the docking experiments. Oligomers are drawn with their reducing end to the right-side of the heptamer.

References

Beukema, M., Faas, M. M., & de Vos, P. (2020). The effects of different dietary fiber pectin structures on the gastrointestinal immune barrier: Impact via gut microbiota and direct effects on immune cells. *Experimental & Molecular Medicine, 52*(9), 1364–1376.

Beukema, M., Jermendi, É., Koster, T., Kitaguchi, K., de Haan, B. J., van den Berg, M. A., & de Vos, P. (2021). Attenuation of doxorubicin-induced small intestinal mucositis by pectins is dependent on Pectin's methyl-Ester number and distribution. *Molecular Nutrition & Food Research, 65*(18), Article 2100222.

Beukema, M., Jermendi, É., Schols, H. A., & de Vos, P. (2020). The influence of calcium on pectin's impact on TLR2 signalling. *Food & Function, 11*(9), 7427–7432.

Beukema, M., Jermendi, É., van den Berg, M., Faas, M., Schols, H., & de Vos, P. (2021). The impact of the level and distribution of methyl-esters of pectins on TLR2-1 dependent anti-inflammatory responses. *Carbohydrate Polymers, 251*, Article 117093.

Blumenkrantz, N., & Asboe-Hansen, G. (1973). New method for quantitative determination of uronic acids. *Analytical Biochemistry, 54*(2), 484–489.

Breton, J., Plé, C., Guerin-Deremaux, L., Pot, B., Lefranc-Millot, C., Wils, D., & Foligné, B. (2015). Intrinsic immunomodulatory effects of low-digestible carbohydrates selectively extend their anti-inflammatory prebiotic potentials. *BioMed Research International, 2015*.

Brownlee, I. A. (2011). The physiological roles of dietary fibre. *Food Hydrocolloids, 25*(2), 238–250.

Broxterman, S. E., & Schols, H. A. (2018). Interactions between pectin and cellulose in primary plant cell walls. *Carbohydrate Polymers, 192*, 263–272.

Chen, E. M., & Mort, A. J. (1996). Nature of sites hydrolyzable by endopolygalacturonase in partially-esterified homogalacturonans. *Carbohydrate Polymers, 29*(2), 129–136.

Daas, P. J., Meyer-Hansen, K., Schols, H. A., De Ruiter, G. A., & Voragen, A. G. (1999). Investigation of the non-esterified galacturonic acid distribution in pectin with endopolygalacturonase. *Carbohydrate Research, 318*(1–4), 135–145.

Daas, P. J., Voragen, A. G., & Schols, H. A. (2000). Characterization of non-esterified galacturonic acid sequences in pectin with endopolygalacturonase. *Carbohydrate Research, 326*(2), 120–129.

Daas, P. J., Voragen, A. G., & Schols, H. A. (2001). Study of the methyl ester distribution in pectin with endo-polygalacturonase and high-performance size-exclusion chromatography. *Biopolymers: Original Research on Biomolecules, 58*(2), 195–203.

DeLano, W. L. (2002). Pymol: An open-source molecular graphics tool. In *, 40(1). CCP4 newsletter on protein crystallography* (pp. 82–92).

Englyst, H. N., & Cummings, J. H. (1984). Simplified method for the measurement of total non-starch polysaccharides by gas-liquid chromatography of constituent sugars as alditol acetates. *Analyst, 109*(7), 937–942.

Ferreira, S. S., Passos, C. P., Madureira, P., Vilanova, M., & Coimbra, M. A. (2015). Structure–function relationships of immunostimulatory polysaccharides: A review. *Carbohydrate Polymers, 132*, 378–396.

Filippov, I. V., & Nicklaus, M. C. (2009). *Optical structure recognition software to recover chemical information: OSRA, an open source solution*. ACS Publications.

Gerschenson, L. N. (2017). The production of galacturonic acid enriched fractions and their functionality. *Food Hydrocolloids, 68*, 23–30.

Grosdidier, A., Zoete, V., & Michielin, O. (2011). SwissDock, a protein-small molecule docking web service based on EADock DSS. *Nucleic Acids Research, 39*(suppl_2), W270–W277.

Guillotin, S., Bakx, E., Boulenguer, P., Mazoyer, J., Schols, H., & Voragen, A. (2005). Populations having different GalA blocks characteristics are present in commercial pectins which are chemically similar but have different functionalities. *Carbohydrate Polymers, 60*(3), 391–398.

Hanwell, M. D., Curtis, D. E., Lonie, D. C., Vandermeersch, T., Zurek, E., & Hutchison, G. R. (2012). Avogadro: An advanced semantic chemical editor, visualization, and analysis platform. *Journal of Cheminformatics, 4*(1), 1–17.

Harmsen, J., Kusters-van Someren, M., & Visser, J. (1990). Cloning and expression of a second aspergillus Niger pectin lyase gene (pelA): Indications of a pectin lyase gene family in A. niger. *Current Genetics, 18*(2), 161–166.

Heri, W., Neukom, H., & Deuel, H. (1961). Chromatographie von pektinen mit verschiedener verteilung der methylester-gruppen auf den fadenmolekeln. 16. Mitteilung über ionenaustauscher. *Helvetica Chimica Acta, 44*(7), 1945–1949. https://doi.org/10.1002/hlca.19610440716

Hu, S., Kuwabara, R., Chica, C. E. N., Smink, A. M., Koster, T., Medina, J. D., & García, A. J. (2021). Toll-like receptor 2-modulating pectin-polymers in alginate-based microcapsules attenuate immune responses and support islet-xenograft survival. *Biomaterials, 266*, Article 120460.

Huisman, M., Oosterveld, A., & Schols, H. (2004). Fast determination of the degree of methyl esterification of pectins by head-space GC. *Food Hydrocolloids, 18*(4), 665–668.

Ishisono, K., Yabe, T., & Kitaguchi, K. (2017). Citrus pectin attenuates endotoxin shock via suppression of toll-like receptor signaling in Peyer's patch myeloid cells. *The Journal of Nutritional Biochemistry, 50*, 38–45.

Jermendi, É., Beukema, M., van den Berg, M., de Vos, P., & Schols, H. (2021). Revealing methyl-esterification patterns of pectins by enzymatic fingerprinting: Beyond the degree of blockiness. *Carbohydrate Polymers, 277*, 118813.

Jin, M. S., Kim, S. E., Heo, J. Y., Lee, M. E., Kim, H. M., Paik, S.-G., & Lee, J.-O. (2007). Crystal structure of the TLR1-TLR2 heterodimer induced by binding of a tri-acylated lipopeptide. *Cell, 130*(6), 1071–1082.

Kiewiet, M. B., Rodríguez, M. I. G., Dekkers, R., Gros, M., Ulfman, L. H., Groeneveld, A., & Faas, M. M. (2018). The epithelial barrier-protecting properties of a soy hydrolysate. *Food & Function, 9*(8), 4164–4172.

Kjøniksen, A.-L., Hiorth, M., & Nyström, B. (2005). Association under shear flow in aqueous solutions of pectin. *European Polymer Journal, 41*(4), 761–770.

Kravtchenko, T., Penci, M., Voragen, A., & Pilnik, W. (1993). Enzymic and chemical degradation of some industrial pectins. *Carbohydrate Polymers, 20*(3), 195–205.

Krieger, E., Joo, K., Lee, J., Lee, J., Raman, S., Thompson, J., & Karplus, K. (2009). Improving physical realism, stereochemistry, and side-chain accuracy in homology modeling: Four approaches that performed well in CASP8. *Proteins: Structure, Function, and Bioinformatics, 77*(S9), 114–122.

Laskowski, R. A., & Swindells, M. B. (2011). *LigPlot+: Multiple ligand–protein interaction diagrams for drug discovery*. ACS Publications.

Leijdekkers, A., Sanders, M., Schols, H., & Gruppen, H. (2011). Characterizing plant cell wall derived oligosaccharides using hydrophilic interaction chromatography with mass spectrometry detection. *Journal of Chromatography A, 1218*(51), 9227–9235.

Levesque-Tremblay, G., Pelloux, J., Braybrook, S. A., & Müller, K. (2015). Tuning of pectin methylesterification: Consequences for cell wall biomechanics and development. *Planta, 242*(4), 791–811.

McKay, S., Oranje, P., Helin, J., Koek, J. H., Kreijveld, E., van den Abbeele, P., & Aparicio-Vergara, M. (2021). Development of an affordable, sustainable and efficacious plant-based immunomodulatory food ingredient based on bell pepper or carrot RG-I pectic polysaccharides. *Nutrients, 13*(3), 963.

Montagne, L., Pluske, J., & Hampson, D. (2003). A review of interactions between dietary fibre and the intestinal mucosa, and their consequences on digestive health in young non-ruminant animals. *Animal Feed Science and Technology, 108*(1–4), 95–117.

Pettersen, E. F., Goddard, T. D., Huang, C. C., Couch, G. S., Greenblatt, D. M., Meng, E. C., & Ferrin, T. E. (2004). UCSF Chimera—a visualization system for exploratory research and analysis. *Journal of Computational Chemistry, 25*(13), 1605–1612.

Popov, S., & Ovodov, Y. S. (2013). Polypotency of the immunomodulatory effect of pectins. *Biochemistry (Moscow), 78*(7), 823–835.

Prado, S. B., Beukema, M., Jermendi, E., Schols, H. A., de Vos, P., & Fabi, J. P. (2020). Pectin interaction with immune receptors is modulated by ripening process in papayas. *Scientific Reports, 10*(1), 1–11.

Ralet, M.-C., Williams, M. A., Tanhatan-Nasseri, A., Ropartz, D., Quéméner, B., & Bonnin, E. (2012). Innovative enzymatic approach to resolve homogalacturonans based on their methylesterification pattern. *Biomacromolecules, 13*(5), 1615–1624.

Ramberg, J. E., Nelson, E. D., & Sinnott, R. A. (2010). Immunomodulatory dietary polysaccharides: A systematic review of the literature. *Nutrition Journal, 9*(1), 54.

Remoroza, C., Buchholt, H., Gruppen, H., & Schols, H. (2014). Descriptive parameters for revealing substitution patterns of sugar beet pectins using pectolytic enzymes. *Carbohydrate Polymers, 101*, 1205–1215.

Remoroza, C., Cord-Landwehr, S., Leijdekkers, A., Moerschbacher, B., Schols, H., & Gruppen, H. (2012). Combined HILIC-ELSD/ESI-MSn enables the separation, identification and quantification of sugar beet pectin derived oligomers. *Carbohydrate Polymers, 90*(1), 41–48.

Renard, C., & Jarvis, M. (1999). Acetylation and methylation of homogalacturonans 2: Effect on ion-binding properties and conformations. *Carbohydrate Polymers, 39*(3), 209–216.

Rösch, C., Taverne, N., Venema, K., Gruppen, H., Wells, J. M., & Schols, H. A. (2017). Effects of in vitro fermentation of barley β-glucan and sugar beet pectin using human fecal inocula on cytokine expression by dendritic cells. *Molecular Nutrition & Food Research, 61*(1), 1600243.

Sahasrabudhe, N. M., Beukema, M., Tian, L., Troost, B., Scholte, J., Bruininx, E., & Schols, H. A. (2018). Dietary fiber pectin directly blocks toll-like receptor 2–1 and prevents doxorubicin-induced ileitis. *Frontiers in Immunology, 9*, 383.

Sahasrabudhe, N. M., Dokter-Fokkens, J., & de Vos, P. (2016). Particulate β-glucans synergistically activate TLR4 and Dectin-1 in human dendritic cells. *Molecular Nutrition & Food Research, 60*(11), 2514–2522.

Sahasrabudhe, N. M., Tian, L., Troost, B., Beukema, M., Scholte, J., Bruininx, E., & Schols, H. A. (2016). Pectin attenuates immune responses by directly blocking Toll-like receptor 2. In *Experimental studies on dietary fibers* (p. 99).

Scharlau, D., Borowicki, A., Habermann, N., Hofmann, T., Klenow, S., Miene, C., & Glei, M. (2009). Mechanisms of primary cancer prevention by butyrate and other products formed during gut flora-mediated fermentation of dietary fibre. *Mutation Research/Reviews in Mutation Research, 682*(1), 39–53.

Shibata, T., Nakashima, F., Honda, K., Lu, Y.-J., Kondo, T., Ushida, Y., & Tanaka, H. (2014). Toll-like receptors as a target of food-derived anti-inflammatory compounds. *Journal of Biological Chemistry, 289*(47), 32757–32772.

Sila, D., Van Buggenhout, S., Duvetter, T., Fraeye, I., De Roeck, A., Van Loey, A., & Hendrickx, M. (2009). Pectins in processed fruits and vegetables: Part II—Structure–function relationships. *Comprehensive Reviews in Food Science and Food Safety, 8*(2), 86–104.

Smith, P. M., Howitt, M. R., Panikov, N., Michaud, M., Gallini, C. A., Bohlooly-Y, M., & Garrett, W. S. (2013). The microbial metabolites, short-chain fatty acids, regulate colonic treg cell homeostasis. *Science, 341*(6145), 569–573.

Takeda, K., & Akira, S. (2005). Toll-like receptors in innate immunity. *International Immunology, 17*(1), 1–14.

Van Gool, M., Van Muiswinkel, G., Hinz, S., Schols, H., Sinitsyn, A., & Gruppen, H. (2013). Two novel GH11 endo-xylanases from myceliophthora thermophila C1 act differently toward soluble and insoluble xylans. *Enzyme and Microbial Technology, 53*(1), 25–32.

Vogt, L., Ramasamy, U., Meyer, D., Pullens, G., Venema, K., Faas, M. M., & de Vos, P. (2013). Immune modulation by different types of β2→ 1-fructans is toll-like receptor dependent. *PloS one, 8*(7), Article e68367.

Vogt, L. M., Meyer, D., Pullens, G., Faas, M. M., Venema, K., Ramasamy, U., & de Vos, P. (2014). Toll-like receptor 2 activation by β2→ 1-fructans protects barrier function of T84 human intestinal epithelial cells in a chain length–dependent manner. *The Journal of Nutrition, 144*(7), 1002–1008.

Vogt, L. M., Sahasrabudhe, N. M., Ramasamy, U., Meyer, D., Pullens, G., Faas, M. M., & de Vos, P. (2016). The impact of lemon pectin characteristics on TLR activation and T84 intestinal epithelial cell barrier function. *Journal of Functional Foods, 22*, 398–407.

Voragen, A., Pilnik, W., Thibault, J., Axelos, M., & Renard, C. (1995). In *Food polysaccharides and their applications* (pp. 287–339). New York: Marcel Dekker, Inc.

Voragen, A., Schols, H., De Vries, J., & Pilnik, W. (1982). High-performance liquid chromatographic analysis of uronic acids and oligogalacturonic acids. *Journal of Chromatography A, 244*(2), 327–336.

Voragen, A. G., Coenen, G.-J., Verhoef, R. P., & Schols, H. A. (2009). Pectin, a versatile polysaccharide present in plant cell walls. *Structural Chemistry, 20*(2), 263.

Voragen, F., Beldman, G., & Schols, H. (2001). In *Chemistry and Enzymology of Pectins* (pp. 379–398). Oxford, UK: Advanced Dietary Fibre Technology. Blackwell Science Ltd.

Voragen, F. (2004). Advances in pectin and pectinase research. *Annals of Botany, 94*(3), 479–480. https://doi.org/10.1093/aob/mch146

Weickert, M. O., Arafat, A. M., Blaut, M., Alpert, C., Becker, N., Leupelt, V., & Pfeiffer, A. F. (2011). Changes in dominant groups of the gut microbiota do not explain cereal-fiber induced improvement of whole-body insulin sensitivity. *Nutrition & Metabolism, 8*(1), 90.

Willats, W. G., Knox, J. P., & Mikkelsen, J. D. (2006). Pectin: New insights into an old polymer are starting to gel. *Trends in Food Science & Technology, 17*(3), 97–104.